Order Number 1336671

Forced ventilation removal of chlorinated hydrocarbons in layered, unsaturated soil material: A laboratory evaluation

Brooks, George Patrick, M.S.

The University of Arizona, 1989

U·M·I
300 N. Zeeb Rd.
Ann Arbor, MI 48106

FORCED VENTILATION REMOVAL OF CHLORINATED HYDROCARBONS IN LAYERED, UNSATURATED SOIL MATERIAL: A LABORATORY EVALUATION

by

George Patrick Brooks

A Thesis Submitted to the faculty of the

DEPARTMENT OF HYDROLOGY AND WATER RESOURCES

In Partial Fulfillment of the Requirements
For the Degree of

MASTER OF SCIENCE
WITH A MAJOR IN HYDROLOGY
In the Graduate College

THE UNIVERSITY OF ARIZONA

1 9 8 9

STATEMENT BY AUTHOR

This thesis has been submitted in partial fulfillment of requirements for an advanced degree at The University of Arizona and is deposited at the University Library to be made available to borrowers under rules of the Library.

Brief quotations from this thesis are allowable without special permission, provided that accurate acknowledgement of the source is made. Requests for permission for extended quotation from or reproduction of this manuscript in whole or in part may be granted by the head of the major department of the Dean of the Graduate College when in their judgement the proposed use of the material is in the interests of scholarship. In all other instances, however, permission must be obtained from the author.

SIGNED: George Patrick Brooks

APPROVAL BY THESIS DIRECTOR

This thesis has been approved on the date shown below:

Daniel D. Evans, Professor of
Hydrology and Water Resources

April 18, 1989
Date

ACKNOWLEDGEMENTS

I want to express my sincere appreciation to my thesis committee. My advisor, Dr. Dan Evans, provided many helpful suggestions, and inspiration when the difficulties were piled high. My co-advisor, Dr. Martha Conklin, always had an open door and time to discuss different analytical approaches relevant to my research. Dr. Todd Rasmussen, while not on my committee, has been involved from start to finish. The laboratory apparatus, and application of the DSC model to unsaturated zone air stripping were Todd's ideas. We refined them together with many discussions and back of the envelope calculations. He was very involved and his help is greatly appreciated.

My wife, Sandra, and our son, Kenny, deserve a big thank you for the patient support they offered while I spent nights away at the office. They gave me the ballast I needed to keep an even keel while at the University of Arizona.

I gratefully acknowledge the assistance of the Salt River Project who partially funded this research.

TABLE OF CONTENTS

TABLE OF CONTENTS--CONTINUED

LIST OF FIGURES

LIST OF FIGURES--CONTINUED

LIST OF TABLES

ABSTRACT

Helium tracer experiments were conducted to characterize conservative tracer behavior in a wedge-shaped lysimeter containing alternating layers of unsaturated silty sand, and clay loam.

Experiments were conducted with trichloroethylene and 1,1,1-trichloroethane to determine if air stripping in unsaturated soil could be characterized by mass transfer from the sorbed to the liquid to the vapor phase. Batch experiments were conducted to measure liquid - vapor mass transfer. Solid - liquid - vapor mass transfer was characterized by measuring the vapor phase re-equilibration after the air stripping experiment.

The Discrete State Compartment model was used to simulate a conservative gas tracer. The results were compared to the helium tracer. Liquid - vapor, and solid -liquid - vapor mass transfer were modeled by fitting simulated data to experimental data. The conservative tracer, and mass transfer models were combined to simulate air stripping in unsaturated soil.

1. INTRODUCTION

1.1 HISTORICAL PERSPECTIVE

As the effect of industrialization on environmental quality and public health is better understood, the number of recognized environmental problems has grown dramatically. The fact that pollutants in the unsaturated zone eventually contaminate ground water has been confirmed by intensive ground water sampling and recent technological advances that increased the measurement sensitivity of many compounds. The soil is no longer thought of as a "living filter". Pollutants enter the unsaturated zone in a variety of ways. Leaky underground storage tanks, surface discharges, spills and surface impoundments contribute to the problem. Petroleum products and chlorinated hydrocarbon solvents are among the most prevalent contaminants of soil and ground water. Many of these pollutants have high vapor pressures at ambient conditions, and are classified as volatile organic compounds (VOCs).

In the vadose zone, a significant fraction of a VOC exists in the vapor phase, and highly concentrated vapor is often denser than air. Diffusion and density driven flow in the soil air pore space are mechanisms that cause VOC vapor to disseminate in the unsaturated zone (Sleep and Sykes,

1989). Dissolution of organic vapor in soil moisture and ground water increases the extent of the original pollution.

In three surveys conducted in 1975, 1977, and 1978 -1979, the U.S. Environmental Protection Agency (USEPA) measured selected VOCs in the drinking water of thirty-nine cities that rely on ground water (USEPA, 1980). The VOC most often detected was trichloroethylene (TCE), a common industrial solvent and degreaser. The USEPA has also estimated that 10 - 30 percent of approximately 3.5 million underground gasoline storage tanks in the United States are leaking (Dowd, 1984). Remedial action is often necessary to remove pollutants where ground water contamination has occurred.

In the last 10 years, air stripping in packed towers utilizing countercurrent flow of air and water has successfully removed VOC's at many locations (Ball et al., 1984; Cline et al. 1985; Hand et al. 1986; Amy et al., 1987). In this strategy, ground water is pumped to the top of a tower and allowed to percolate through packing material which maximizes the liquid - vapor interface. Clean air is forced through the tower and dissolved contaminants vaporize into the air stream. Packed tower air stripping relies on pollutant mass transfer from the liquid to the vapor phase. Therefore, VOCs are well suited to this removal strategy.

By extending air stripping technology to the unsaturated zone, pollutants can be removed before they reach the water table. In the unsaturated zone, VOCs may exist in up to four

phases. VOCs may be present as a free product, dissolved in soil water, as a vapor, or sorbed to the soil material (organic carbon content). The ratio of (vapor phase : aqueous phase : sorbed phase) is controlled by soil porosity, degree of saturation, fraction soil organic content, and equilibrium partitioning between the liquid, solid, and vapor phases.

At equilibrium, the chemical potentials of all phases are equal, and net mass transfer does not occur. When clean air is forced into soil air pore space, it mixes with the VOC vapor thereby lowering the vapor phase concentration and, therefore the chemical potential. This induces a mass transfer from the liquid to the vapor, and in turn a transfer from the sorbed phase to the aqueous phase occurs. Continuing this process will eventually remove VOCs from the soil. Factors that influence the removal rate of VOCs from unsaturated soil include temperature, forced ventilation rate, soil permeability, porosity, degree of saturation, equilibrium partitioning, and rates of mass transfer between the phases. Different processes may be rate limiting at different stages in the air stripping process.

The organic vapor that is removed from the soil may be incinerated, sorbed in filters of activated carbon and other sorbents, or vented directly to the atmosphere.

There have recently been many successful attempts at air stripping in the unsaturated zone. A characteristic scenario begins with initial rapid extraction of VOCs followed by a

long time period with smaller removal rates (Hoag et al. 1987; Crow et al. 1987; Bruckner et al., 1986.) The rapid extraction step may represent removal of organic vapor from the soil air pore space, desorption from the aqueous phase and initially fast desorption from the solid phase. The rate of forced ventilation is important during the initial step to facilitate rapid removal. The nature of the slower removal rate is likely tied to mass transfer between the solid, liquid, and vapor phases, and will be explored in this investigation.

1.2 PREVIOUS LABORATORY AND FIELD STUDIES

Marley (1985) investigated forced ventilation of sand residually saturated with gasoline in plexiglass columns. For 27 experimental runs, the total gravimetrically measured mass removal of gasoline was 100 ± 1 percent.

Researchers at the Texas Research Institute (1982, 1984) conducted soil venting experiments in a large scale model aquifer (20' x 10' x 4') composed of washed river sand (1982, 1984). Gasoline was allowed to accumulate above the water table, and varied well geometries and air flow rate to determine the effect on the soil venting process. Removal efficiency was found to be enhanced by increasing the ventilation rate, and reducing the well spacing. At the highest rate of flow (5.3 scfm), 57 percent of a 75 gallon spill was removed in 11 days.

Crow et al. (1987) conducted pilot-scale experiments to determine the efficacy of controlling and eliminating hydrocarbon vapors from an unsaturated sand formation above a zone of gasoline-saturated soils. The most significant reduction in hydrocarbon vapor occurred during the first 1 to 3 days. During a 14 day re-equilibration period, the average hydrocarbon concentration returned to 62 percent of the average baseline concentration. It was observed that the time required to reduce hydrocarbon vapor in the unsaturated zone was shorter than the time required for vapor concentrations to re-establish to original baseline levels. The induced pressure within the soil was measured and radial area of influence around the vapor recovery wells was determined. In each case, the static pressure was observed to decrease exponentially with an increase in radial distance.

Hoag et al. (1987) used the soil venting process to remediate a gasoline spill estimated at 320 to 420 gallons. Three vacuum pumps were operated for 90 days, and 364 gallons of gasoline was recovered. Of the amount removed, 90 percent was recovered in the first 40 days.

Bruckner et al. (1986) published an account of in situ soil ventilation to remove TCE. The first 20 to 30 days were characterized by removal rates greater than 20 kilograms per day, followed by a second stage of reduced efficiency where removal rates dropped to less than 5 kilograms per day.

1.3 STATEMENT OF PURPOSE

The hypothesis investigated in this research was that mass transfer between VOC sorbed phase, dissolved phase, and vapor phase could be used to characterize air stripping in unsaturated soil. Data collected from laboratory experiments were used to validate a computer model that simulated air stripping in unsaturated soil. The objectives of this investigation were:

1) to determine the mass transfer characteristics of TCE and 1,1,1-TCA in unsaturated soil,
2) identify those soil properties which influence air stripping efficiency, and
3) simulate the air stripping process with the Discrete State Compartment (DSC) model by including mass transfer between the solid, liquid, and vapor phases.

This study utilized a wedge-shaped lysimeter containing four alternating layers of silty sand, and clay loam to examine the process of air stripping in layered, unsaturated soil. Helium tracer tests were conducted to calibrate the DSC model for a conservative vapor phase tracer. To simulate the air stripping process it was assumed that each soil grain was enveloped by a film of water, and that mass transfer did not occur directly from the soil surface to the soil atmosphere. Instead, transfer took place between the solid (soil organic matter) and liquid, and between the liquid and vapor phases.

Initially, equilibrium conditions were assumed to exist. The organic compounds were compartmentalized by phase using estimates of equilibrium partitioning coefficients from the literature. Mass transfer rates were measured in the laboratory, and converted to exchange parameters for use in the DSC model. The model simulated radial, forced ventilation of unsaturated soil with clean air. Disequilibrium conditions were produced when clean air mixed with organic vapor in the soil air pore space. This initiated mass transfer from the liquid to vapor, and in turn, from solid to liquid. The vapor was advected out of the system.

The data collected during the air stripping experiments were used to validate the DSC model mass transfer algorithms, and conclusions were drawn about possible applications of the DSC model for field conditions. Figure 1.1 illustrates the conceptual mass transfer model, and the DSC model algorithm that was used to simulate it.

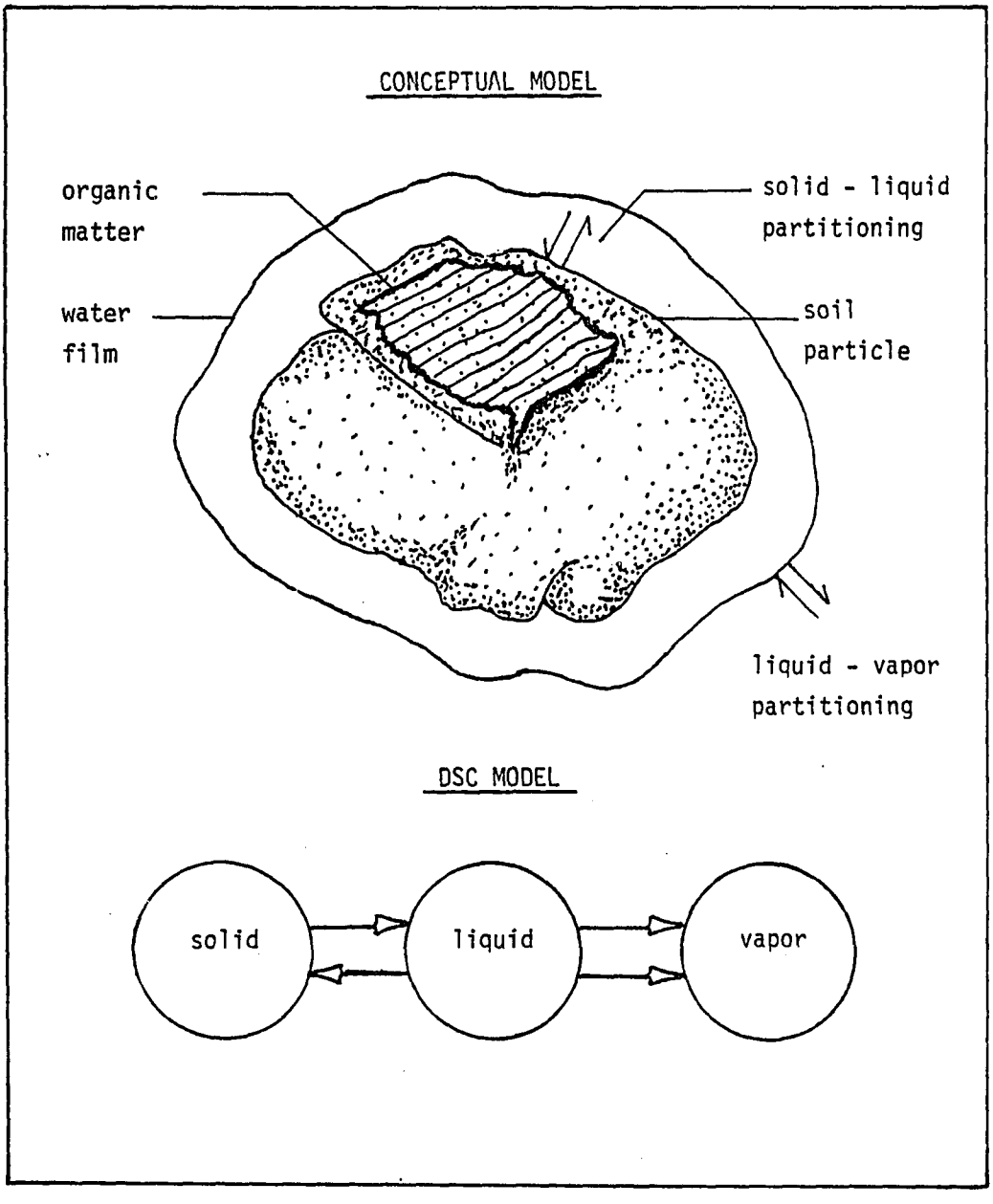

Figure 1.1. The conceptual mass transfer model has a film of water surrounding each soil grain, and does not allow direct solid - vapor mass transfer. The DSC model simulates the conceptual model by compartmentalizing the VOC by phase, and preventing direct mass transfer between the solid and vapor phases.

2. THEORETICAL CONSIDERATIONS

2.1 LIQUID - VAPOR EQUILIBRIUM PARTITIONING

In this investigation it was assumed that the soil contained TCE and 1,1,1 TCA in three phases (i.e. sorbed to solids, dissolved in water, and as a vapor). At equilibrium, the relative fraction of VOC in each phase is expressed by its liquid - vapor, and solid - liquid partitioning coefficients. Henry's Law states that in dilute solutions the vapor pressure of a solute is proportional to its molar concentration. Henry's Law is assumed to hold for TCE and 1,1,1-TCA because both are sparingly soluble in water. The respective solubilities are 1080 and 1550 mg/l (Horvath, 1982). Henry's Law is commonly expressed as:

$$p = K_h C_l \qquad (2.1)$$

where p = partial pressure (atm)

K_h = Henry's constant (atm m^3 mol^{-1})

C_l = aqueous concentration (mol m^{-3})

Using the ideal gas law, Equation 2.1 can be rewritten to produce a dimensionless Henry's constant by:

$$H_c = p / RTC_l Mw \qquad (2.2)$$

where H_c = dimensionless Henry's constant (cm^3 water cm^{-3} air)

R = gas constant (cm^3 atm K^{-1} mol^{-1})

T = absolute temperature (K)

C_l = aqueous concentration (mg cm^{-3} water)

Mw = molecular weight (mg mol^{-1})

H_c can be calculated using the saturation vapor pressure and the aqueous solubility. This method suffers from the lack of reliable solubility data. For example, reported solubility values for TCE range from 700 - 2640 mg/l. Also, the vapor pressure of an organic compound in a water saturated system may be different from that of the pure compound. It is the latter value which is usually reported in the literature.

Recently, Munz and Roberts (1987) conducted experiments to measure the temperature dependence of the Henry's constant on a variety of nonionic halogenated organic compounds in a water saturated system. The temperature dependence of the Henry's constant is described by:

$$\log H_c = A - B/T \qquad (2.3)$$

where A,B = regression coefficients

A linear least-squares regression was made and regression coefficients for Equation 2.3 were obtained for temperatures between 10 °C and 30 °C. For TCE, A = 6.026 and B = 1909.

For 1,1,1-TCA, A = 5.327 and B = 1636.

Gossett (1987) performed a similar study using a modification of the EPICS procedure (Equilibrium Partitioning in Closed Systems). Results were obtained from the measurement of vapor concentration ratios from pairs of sealed vials containing different liquid volumes. Figure 2.1 illustrates that similar results were obtained by Munz and Roberts (1987), and Gossett (1987). The values obtained by Gossett were used in this investigation. At 20 °C, H_c for TCE is 0.308, and for TCA it is 0.570.

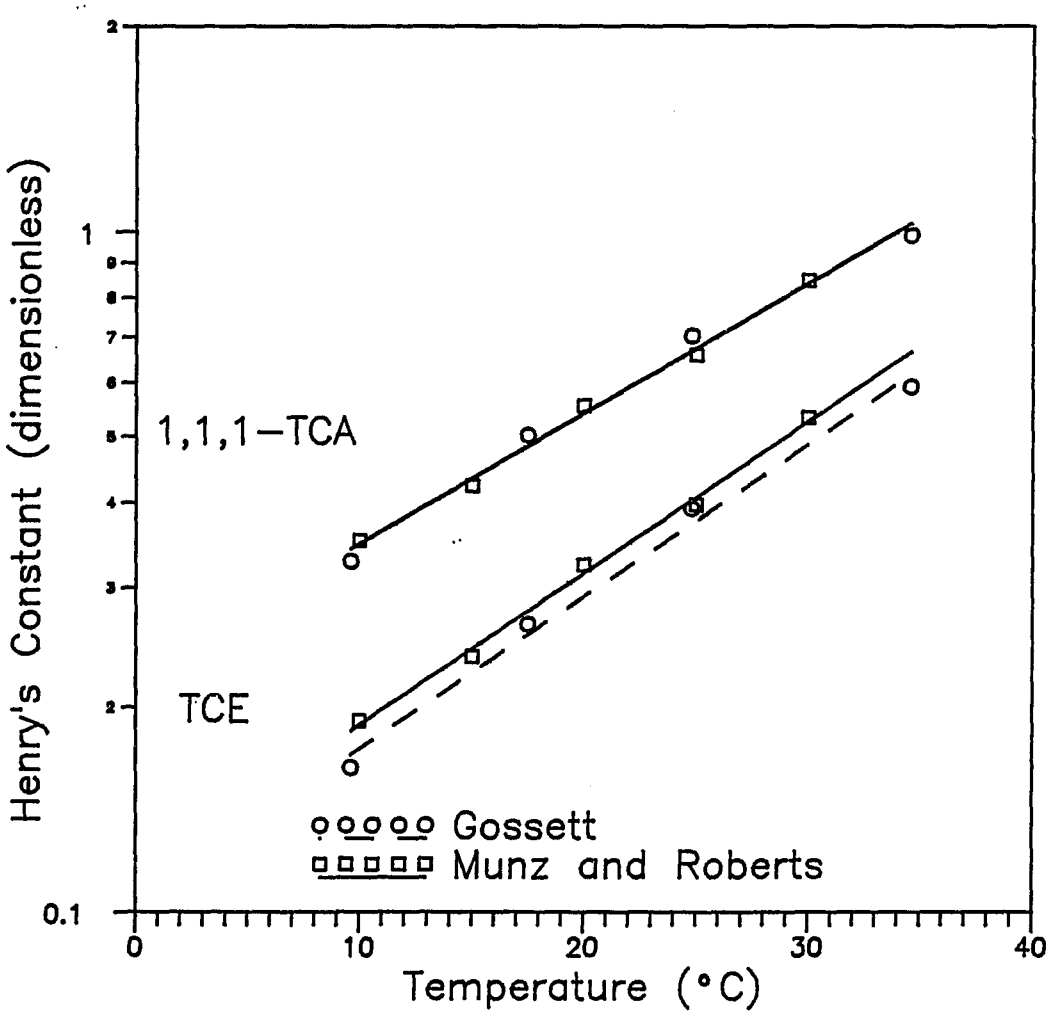

Figure 2.1. The dimensionless Henry's constants determined in separate investigations for TCE and 1,1,1-TCA are very similar.

2.1.1 SOLID - LIQUID EQUILIBRIUM PARTITIONING

The solid - liquid partitioning coefficient describes the equilibrium ratio of the sorbed concentration to the aqueous concentration. In a two phase solid - liquid system, sorption of nonionic organic compounds can be written:

$$S = K_p C_l \qquad (2.4)$$

where S = sorbed concentration (mg g^{-1} soil)

K_p = solid - liquid partitioning coefficient (cm^3 water g^{-1} soil)

C_l = aqueous concentration (mg cm^{-3} water)

Schwarzenbach and Westall (1981) observed linear sorption isotherms for several hydrophobic organic compounds partitioning between sediment and water. They noted that the extent to which a compound partitions to the solid phase is dependent on the fraction of organic material in the soil. A highly significant correlation was found between the logarithms of the average K_{OC} values and the logarithms of the K_{OW} values ($r^2 = 0.95$). It was described by:

$$\log K_{OC} = 0.72 \log K_{OW} + 0.49 \qquad (2.5)$$

where K_{OC} = (hypothetical) partitioning coefficient for adsorbent that is 100% organic carbon

K_{OW} = octanol - water partitioning coefficient

For a sorbent that is not 100% organic material, the partitioning coefficient was found by:

$$\log K_p = 0.72 \log K_{OW} + \log f_{OC} + 0.49 \qquad (2.6)$$

where f_{OC} = mass fraction of soil organic carbon

Chiou and Shoup (1985) conducted experiments with several nonionic organic compounds to determine the effect of relative humidity on the sorption of organic vapor on dry soil. They found that sorption on dry soil was nonlinear and much higher than for aqueous systems. It was proposed that soil behaved as a dual sorbent in which the organic compounds sorbed both to the mineral fraction, and the organic matter. As relative humidity increased, sorption was observed to decrease. At 90% relative humidity the sorption isotherms for some compounds closely matched those for a saturated system. It was hypothesized that the more polar water vapor displaced the organic vapor from sorption sites on soil minerals. At high relative humidities, the sorption of organic vapor to soil minerals was effectively inhibited, and partitioning with soil organic matter was the dominant sorption mechanism. Since the relative humidity in unsaturated soil is near 99% even at large negative moisture potentials (Hillel, 1980), the

relationship that describes solid - liquid partitioning of nonionic organic compounds in saturated systems can be used as an approximation in unsaturated systems.

Peterson et al. (1988) conducted solid - vapor sorption experiments with simulated soil material composed of alumina oxide coated with humic acid. The resulting f_{oc} was 0.48. The synthetic soil was hydrated by exposing it to water vapor, and then allowing it to equilibrate in a closed chamber for 3 days. Water contents of 8.2 percent and 11.2 percent (g H_2O / g solid) were achieved. They found that TCE sorption isotherms in unsaturated material were two orders of magnitude greater than in the saturated system. However, Malcom and MacCarthy (1986) caution that commercial humic acids are not representative of humic and fulvic acids found in soils.

Both the results of Chiou and Shoup (1985) and Peterson et al. (1988) indicate that the value obtained for K_p in a saturated system could be considered the lower limit for K_p in unsaturated soil.

2.2 LIQUID - VAPOR MASS TRANSFER KINETICS

At equilibrium, the chemical potentials of all phases are equal and no net mass transfer occurs. The driving force of mass transfer between phases is a chemical potential gradient. If an imbalance exists, mass transfer occurs down gradient until equilibrium is reached. Treybal (1980) used the two-resistance theory to describe liquid - vapor

partitioning. The two-resistance theory assumes that diffusional resistance exists in the liquid and vapor, but not in the interface that separates them. At the interface, the chemical potential of liquid and vapor is assumed to be equal. Mass transfer across the interface can be expressed in terms of an overall mass transfer coefficient which is related to the sum of the individual diffusional resistances of both phases. The time rate of change of the aqueous concentration can be written:

$$dC_l/dt = \alpha_w \left((C_a/H_c) - C_l \right) \qquad (2.8)$$

where α_w = liquid - vapor mass transfer rate coefficient (s^{-1})

McKay and Leinonen (1975) demonstrated that liquid - vapor mass transfer in substances with high Henry's constants (i.e. above 1.6×10^{-1} atm m^3/mol) was controlled by the liquid phase diffusional resistance. Conversely, mass transfer in compounds with a smaller Henry's constant was controlled by vapor diffusional resistance.

Roberts and Dändliker (1983) confirmed that liquid diffusional resistance controlled mass transfer for TCE and 1,1,1-TCA. They used an agitated vessel container to cause turbulence in the air phase above aqueous solutions of six organic compounds. They found that mass transfer from the

aqueous to air phase was not enhanced by vapor agitation for TCE and 1,1,1-TCA.

2.2.1 SOLID - LIQUID MASS TRANSFER KINETICS

Many researchers have reported two stage sorption - desorption kinetics in water - sediment systems (Leenheer and Ahlrichs, 1971; Karickhoff, 1980, 1984; Freeman and Cheung, 1981; and Wu and Gschund, 1986). An initial fast rate is theorized to be sorption or desorption from the solid surface, and the slower rate is attributed to diffusion through the solid. Freeman and Cheung (1981) assumed that the sorptive properties of a sediment are due primarily to its organic content (humin - kerogen). The humin - kerogen structure is pictured as consisting of highly branched polymer chains that form a three-dimensional, randomly oriented network bound to a soil mineral substrate. A liquid adsorbed by the structure causes the network to swell and form a gel. Different liquids induce different degrees of swelling. By experimenting with different fluids and therefore, different degrees of swelling, the researchers noted that the slow desorption step for a given compound was accelerated when the gel was more swollen. It follows that solute diffusion through a swollen gel should be faster than through a denser one.

Another study that supports the theory that sorption kinetics are controlled by intra-particle diffusion was conducted by Wu and Gschwend (1986). They developed a radial

diffusion model based on chemical and particle properties that agrees well with experimental desorption data.

Mass transfer from solid to liquid is similar to equation 2.8. The aqueous concentration is adjusted by K_p to express a chemical potential gradient. For a single mass transfer rate, the change in solid concentration with time is written:

$$dS/dt = \alpha_s \ (K_p C_1 - S) \qquad (2.9)$$

where α_s = solid - liquid mass transfer rate coefficient (s^{-1})

If two parallel mass transfer rates are present, equation 2.9 can be rewritten by:

$$\delta S/\delta t = \alpha_1 \ (K_p C_1 - S_1) + \alpha_2 \ (K_p C_1 - S_2) \qquad (2.10)$$

where α_1 = rate coefficient for process 1 (s^{-1})

α_2 = rate coefficient for process 2 (s^{-1})

S_1 = fraction of VOC affected by rate 1

S_2 = fraction of VOC affected by rate 2

2.3 SOIL AIR PERMEABILITY

Assuming that large scale heterogeneities are absent (i.e. root holes, animal burrows, or soil cracks), the air permeability of unsaturated soil is controlled by soil

porosity, pore geometry, and degree of saturation, For radial, incompressible, laminar flow in a homogeneous porous media vapor movement is described with Darcy's Law (Muskat, 1946) by:

$$q = -k/\mu \, dP/dr \qquad (2.11)$$

where k = intrinsic permeability (cm^2)

P = pressure (dyne cm^{-2})

μ = dynamic viscosity (g cm^{-1} s^{-1})

r = radial distance (cm)

For the case where compressible flow occurs, an additional term that represents the contribution to flow by expanding gas (Kilbury et al.,1986) is added to the flow equation by:

$$q = -k/\mu \, dP/dr - kdP^2/2\mu P_o dr \qquad (2.12)$$

where P_o = reference pressure (atm)

The incompressible, volumetric flow rate from an injection or extraction well in radial coordinates is written:

$$Q = 2\pi rh \, k/\mu \, dP/dr \qquad (2.13)$$

where h = height of well gravel pack (cm)

The Theim equation can be adapted to solve for soil air conductivity. Separating variables and integrating Equation 2.9 yields:

$$\ln r_2/r_1 = 2\pi hk/\mu Q\ (P_2 - P_1) \qquad (2.14)$$

This intermediate step shows that for radial air flow, the graph of P vs. ln r is a straight line with a slope equal to the constant $2\pi hk/uQ$. Equation 2.10 can be rewritten to solve for soil air conductivity as:

$$K_a = k\Omega g/\mu = \ln r_2/r_1 \quad Q/2\pi h(H_2 - H_1) \qquad (2.15)$$

where K_a = soil air permeability (cm/s)

$P_2 - P_1 = g(H_2 - H_1)$

Ω = density of fluid in manometer

g = gravitational acceleration

H_1 = static manometer fluid level (cm)

H_2 = pressurized manometer fluid level (cm)

2.4 ADVECTION - DISPERSION PARADIGM

The spreading out of the VOC vapor concentration profile of a VOC in the unsaturated soil is caused by mechanical dispersion, and molecular diffusion. The combination of these terms is called hydrodynamic dispersion. The dimensionless Peclet number is used to express the relative importance of

each term. Freeze and Cherry (1979) describe it for saturated flow by:

$$P_e = qd/D_m \qquad (2.16)$$

where P_e = Peclet number

q = linear velocity (cm s^{-1})

d = average particle diameter (cm)

D_m = molecular diffusion coefficient (cm^2 s^{-1})

At low velocity the Peclet number is small, and hydrodynamic dispersion is dominated by molecular diffusion. In a very fine grained soil such as the confining layer in the experimental model, diffusion is more significant. The Peclet number is large at high velocity, and mechanical dispersion is more important.

In unsaturated soil, the change of VOC concentration with time due to air stripping can be described by coupling the advection - dispersion equation with chemical rate equations. The relationship is expressed by:

$$\Theta_a\, \delta C_a/\delta t + \Theta_w\, \delta C_l/\delta t + (1-\Theta_a-\Theta_s)\, \delta S/\delta t = \qquad (2.17)$$
$$\Theta_a D_a \left((\delta/r\delta r)(r\delta C_a/\delta r) - q(r)\delta C_a/\delta r \right)$$

where Θ_a = air filled porosity (cm^3 air cm^{-3} porous media)

Θ_w = water filled porosity

(cm^3 water cm^{-3} porous media)

D_a = hydrodynamic dispersion coefficient (cm^2 s^{-1})

$q(r)$ = linear air velocity as a function of r

(cm s^{-1})

$$\delta C_l/\delta t = \alpha_w \left((C_a/H_c) - C_l \right)$$

$$\delta S/\delta t = \alpha_s (K_p C_l - S)$$

There is not an analytical solution available for equation 2.17. The DSC model was used to approximate a solution by combining conservative tracer simulation with desorption rates measured in the laboratory.

3. LABORATORY APPARATUS

3.1 MODEL CONSTRUCTION

A wedge-shaped lysimeter was constructed to simulate the conditions of radial forced ventilation in unsaturated soil. A triangular plexiglass prism with internal angles of 60 degrees was built with sides of 1 meter each, and a height of 1 meter. The model shape was meant to represent a segment of an axially symmetric flow field. Figure 3.1 is an illustration of the laboratory apparatus.

The lysimeter was constructed with 1/4 inch plexiglass sheets fastened with machine screws every 5 inches. Weld-on #3, a mixture of methylene chloride and TCE (Industrial Polychemical Service, Los Angeles, Ca.), was used to bond the plexiglass sheets together. The mixture was applied to the seams with a small brush, and capillary force caused the solvent to spread across the joint interface. Machine screws were then tightened, and a secure bond was formed. The seams were sealed with at least 2 layers of Formagasket #2 (Locktite Corp., Mississaugua, Ontario). The removable plexiglass top was sealed with silicone sealant and fastened with machine screws. A supporting frame of 1½" x 1½" x 1/8" angle iron was constructed around the model.

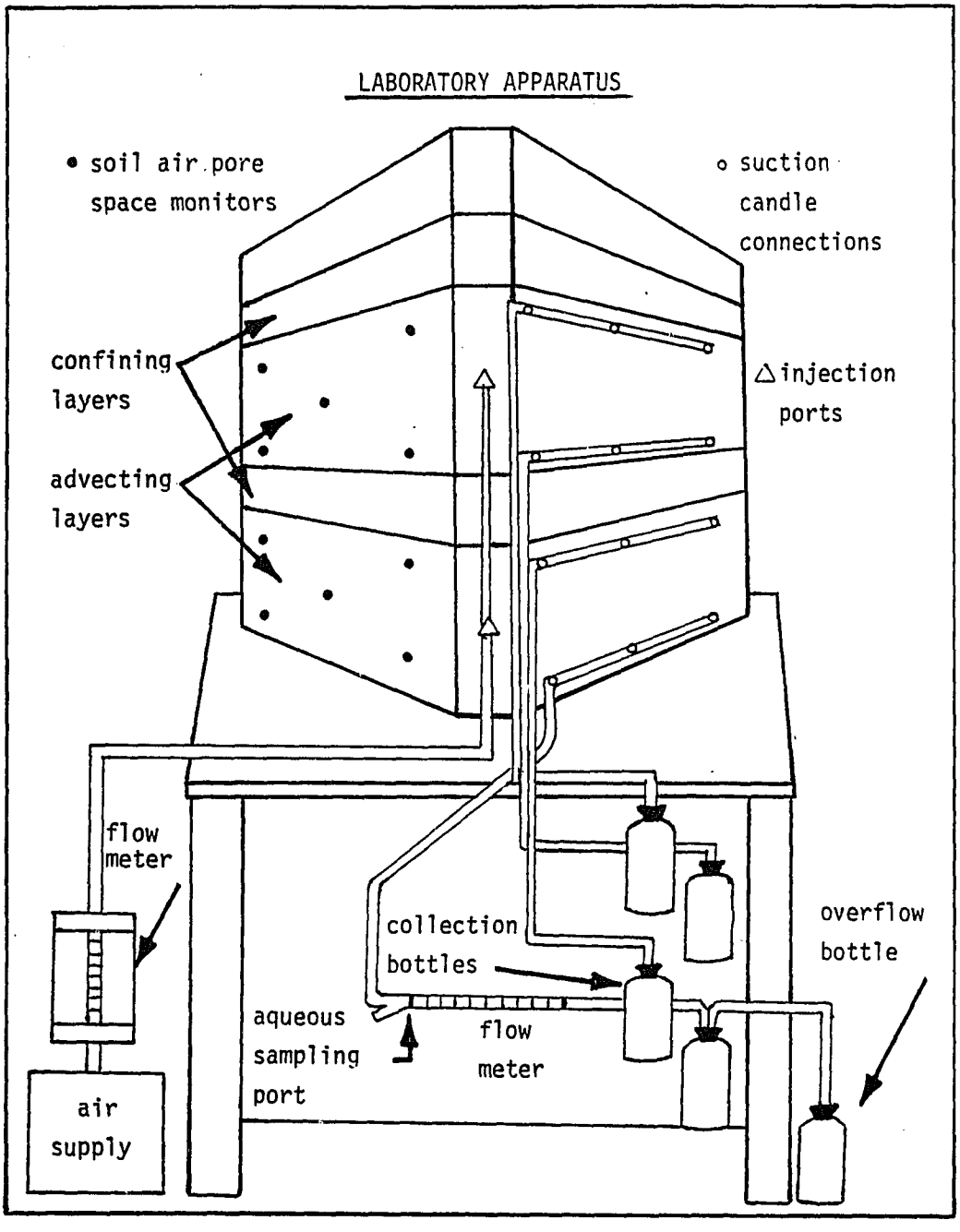

Figure 3.1. Illustration of the laboratory apparatus used to conduct air stripping experiments in unsaturated soil material.

To eliminate the possibility of preferential air flow along the sides of the enclosure, a medium to coarse grained sand was glued to the plexiglass with Locktite 330 Depend (Locktite Corp.). Soil particles would then make direct contact with the irregular surface formed by the sand, and air would not be likely to flow preferentially between the soil and the plexiglass walls. 1,1,1 TCA was an active ingredient in Locktite 330 Depend. It was unintentionally introduced into the system by way of the adhesive.

3.1.1 SOIL MATERIAL

Two types of soil material were used in this investigation to provide a layering effect in the model. Soil A was a composite sample taken from a depth of 0 to 20 feet from a site in Phoenix, Arizona. Soil A was dry sieved and the +2 mm fraction was discarded. The remaining sample was classified as a yellowish brown, silty fine to medium sand. Soil B (Avondale Clay Loam) was taken from the University of Arizona's Prince Road Farm. Both soils were tested for total organic carbon (mass fraction) by Desert Analytics, Inc., Tucson, Arizona. Soil characteristics are presented in Table 3.1.

PROPERTIES OF SOIL MATERIAL USED IN LABORATORY MODEL

Soil Characteristics	Soil A	Soil B
Sand	72%	0%
Silt and Clay	28%	100%
Fraction Organic Carbon	0.0012	0.0012
Bulk Density (g cm^{-3})	1.54	1.60
Porosity	0.42	0.4
Percent Saturation	0.35	0.63
Intrinsic Permeability (cm^2)	7.3×10^{-7}	1.0×10^{-9}

Table 3.1. Physical properties of the experimental soils material and percentages of liquid, vapor, and organic carbon are listed for each soil type.

3.1.2 SOIL LAYERING

Figure 3.2 illustrates the soil layering with a side view of the model. Soil A formed the bottom layer. It was 30 cm thick and weighed 491 pounds. Soil A was compacted at a water content of 3 percent by weight.

Soil B formed the second layer. It was 10 cm thick and weighed 186 pounds. Soil B was compacted at its optimum moisture content for compaction (12.5 percent) as determined by the ASTM maximum soil density test.

A layer of soil A followed. It was 18 cm thick and weighed 325 pounds with 3 percent by weight water.

The top layer was soil B. It also was 10 cm thick and weighed 195 pounds with 12.5 percent by weight water.

In later experiments, a plastic sheet was spread across the top soil layer, and sealed to the plexiglass with silicone sealant. This prevented vapor diffusion through the soil into the model atmosphere. Approximately 2 inches of water was ponded on the plastic surface to prevent ballooning.

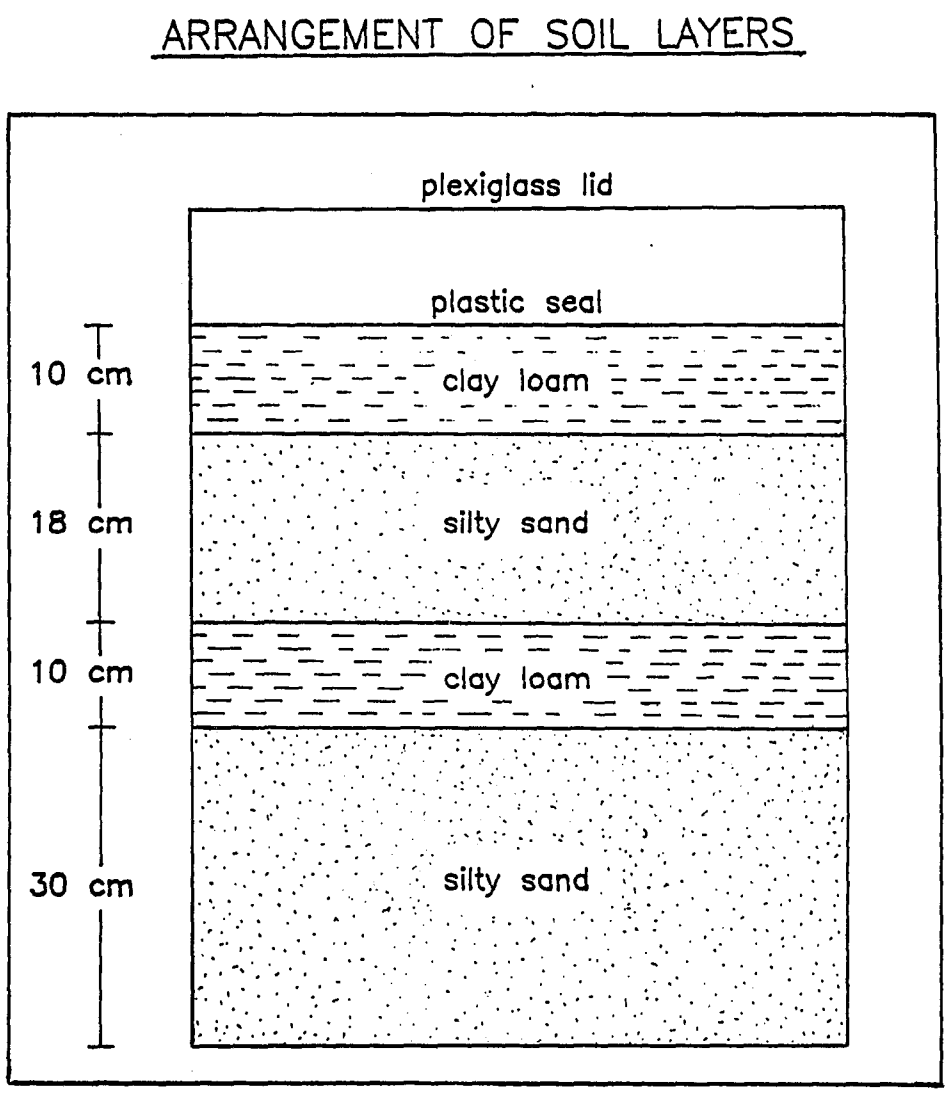

Figure 3.2. Side view of model illustrates soil layering in laboratory apparatus.

3.1.3 AIR DISPERSION

The apex of the lysimeter was used as an air injection port. To enhance the even dispersion of air into the soil at the injection port, pea gravel was backfilled concurrently with the placement of the soil A layers. Figure 3.3 is a plan view of the pea gravel placement in soil A layers. Pea gravel was also backfilled at the model exit ports in the soil A layers. During backfilling, the pea gravel was separated from the soil by an appropriately shaped piece of metal screen (i.e. shaped in the form of an arc for the injection port, and a rectangle for the exit ports). Soil B layers did not contain any of the dispersing gravel. It was intended to serve as a confining layer.

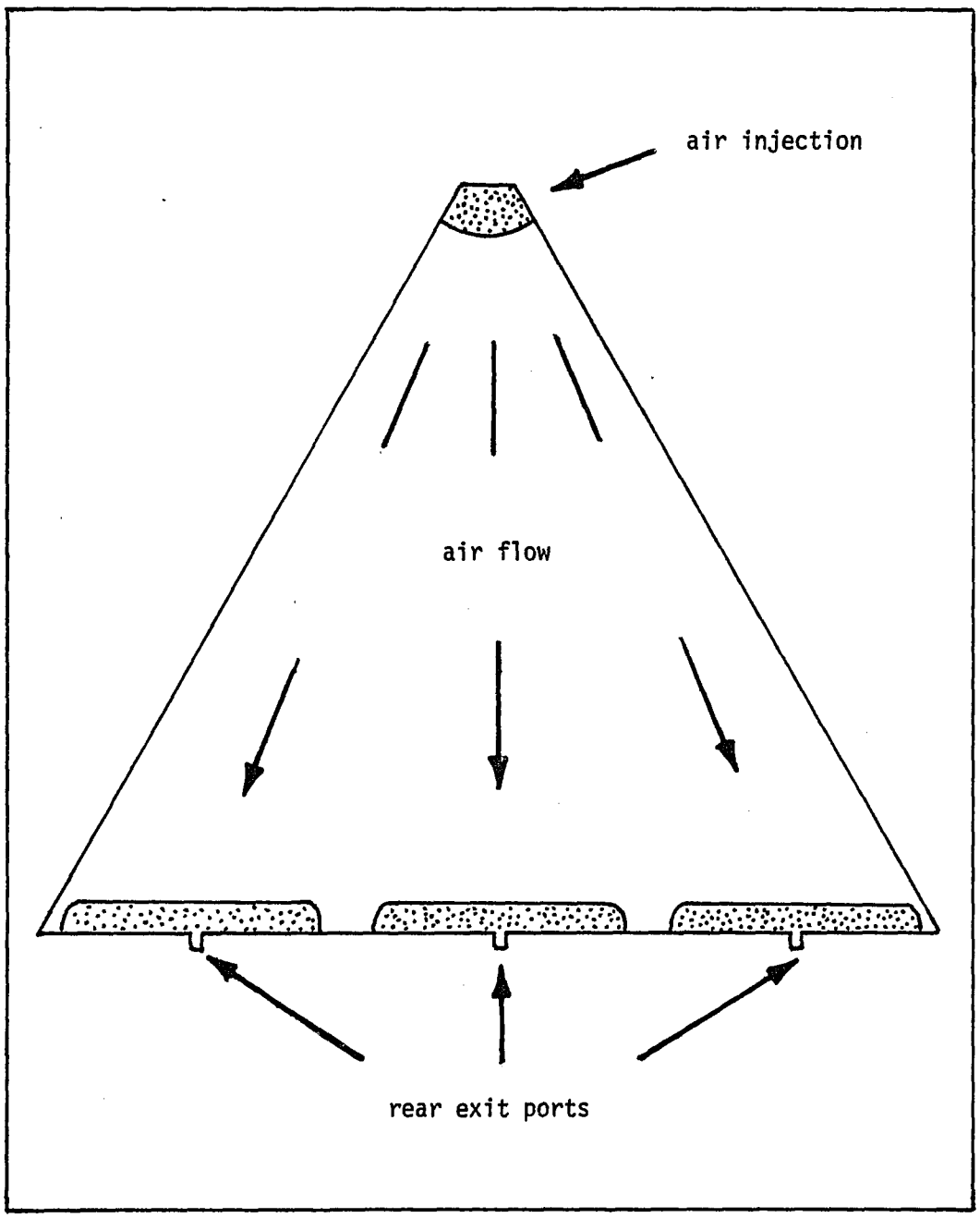

Figure 3.3. Pea gravel was used to disperse air into and out of the advecting soil layer. The plan view diagram illustrates the location of pea gravel backfill.

3.1.4 SOIL MOISTURE CONTROL

To simulate unsaturated conditions, three 12" x 1" cylindrical suction candles were placed at the top and bottom of the soil A layers. The suction candles were manufactured with a porous ceramic material that allowed the free movement of water, but prevented the passage of air. This arrangement enabled water in the suction candles to equilibrate with the soil moisture potential. To maintain a constant soil moisture potential, a negative potential of 80 cm of H_2O was imposed on the suction candles with a column of water 80 cm long contained by tygon tubing. The top of the column was connected to the top of the suction candle, and the bottom was placed in a 1 liter bottle partly filled with water. Soil moisture potential then equilibrated with the potential in the suction candles. With no matric potential gradient, only the gravity gradient induced unsaturated flow. The gravity gradient caused soil moisture to flow from top to bottom, and therefore, soil moisture potential in the upper layer decreased. This caused water to flow from the collection bottle to the suction candles and into the soil. Moisture content of the soil in the bottom layer increased as a result of gravity induced flow. This caused soil water to flow into the suction candles which drained into a collection bottle.

Soil water was continuously recycled in the model. All bottles were sealed with rubber stoppers to prevent vapor from entering the laboratory. The headspace of each bottle was

connected to activated carbon filters (discussed in 3.1.6).

Flow from the 3 bottom suction candles was routed through a volumetric flow meter so an effective unsaturated hydraulic conductivity could be calculated. A sampling port with a rubber septa was installed upstream of the flow meter to facilitate aqueous sampling with a hypodermic syringe. Aqueous samples were injected into sealed vials to permit analysis of the sample headspace.

3.1.5 VAPOR TREATMENT SYSTEM

Activated carbon filters were constructed to reduce the discharge of TCE and 1,1,1 TCA to the atmosphere. The granular carbon used in the filters is marketed by Cameron-Yakima, Inc., Yakima, Wa. It has a specific surface of 1100 m^2 per gram, and is specifically designed for vapor phase adsorption. Adsorption of TCE and 1,1,1 TCA takes place primarily in the carbon micropores. Water vapor is also adsorbed in the micropores, and reduces filter efficiency. Four filters were connected in series so the majority of adsorption took place in the first filter. The carbon could be replaced when it became saturated.

3.1.6 SOIL AIR PORE SPACE MONITORING

Ten soil air pore space monitors were installed at uniformly distributed locations within soil A. They consisted of 5/16" O.D. tygon tubing leading to a 1" piece of 5/16 I.D.

tygon tubing filled loosely with pyrex wool. Loose packing was necessary to prevent soil moisture from entering the monitoring ports. Vapor concentration and soil air pressure were measured with the soil air pore space monitors.

To provide a sealable opening in the model, a hole slightly smaller than the tubing O.D. was drilled in the plexiglass. The tubing was drawn through the opening and glued with Locktite 330 Depend. To sample the vapor without interrupting the flow field, rubber septa were fit onto the tubing. The septa were suitable for repeated puncture with a sampling syringe. The locations of the suction candles and vapor sampling ports is illustrated in Figure 3.4.

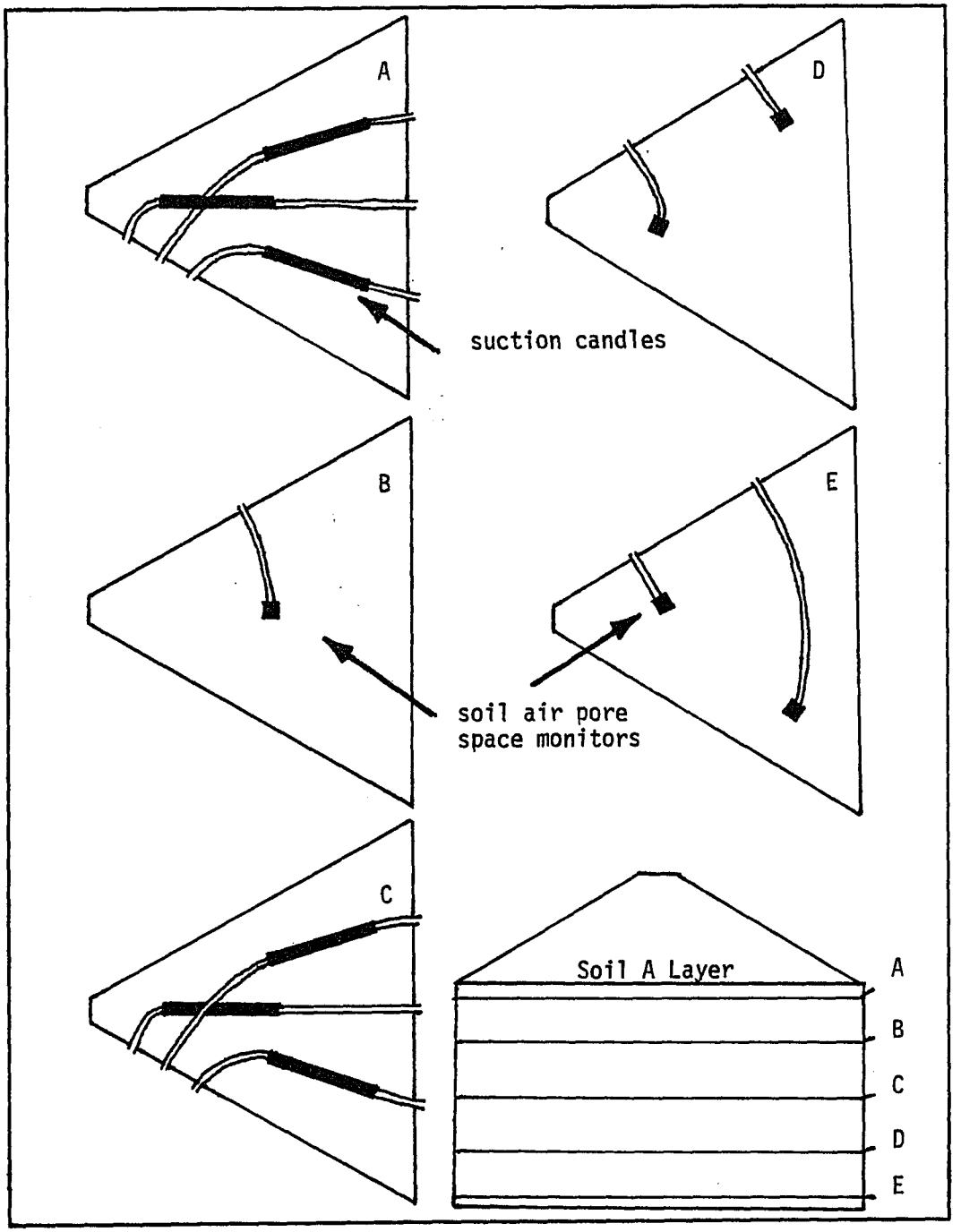

Figure 3.4. Placement of suction candles and air pore space monitoring ports are illustrated in plan view. Letters A through E mark the vertical position in the soil layer.

4. LABORATORY EXPERIMENTS

4.1 AIR FLOW CHARACTERIZATION

The flow characteristics of the model were intended to simulate radial air flow of an operating injection or extraction well in unsaturated soil. Several experiments were conducted to determine the pressure field within the soil in response to applied suction and injection of air. To facilitate pressure measurements, the soil air pore space monitors were connected to water manometers. Soil air pressure at different radial distances from the origin were measured. Equation 2.10 states that pressure decreases exponentially with an increase in radial distance. The pressure data were plotted against ln r to determine if the model was simulating radial, incompressible air flow. Pressure drop with increase in radial distance conformed with Equation 2.10 in all cases. Additionally, helium breakthrough curves measured at the three rear exit ports indicated that preferential air flow did not exist between the apparatus walls and the soil. Figure 4.1 is a graph of soil air pore space pressure vs. the natural log of radial distance.

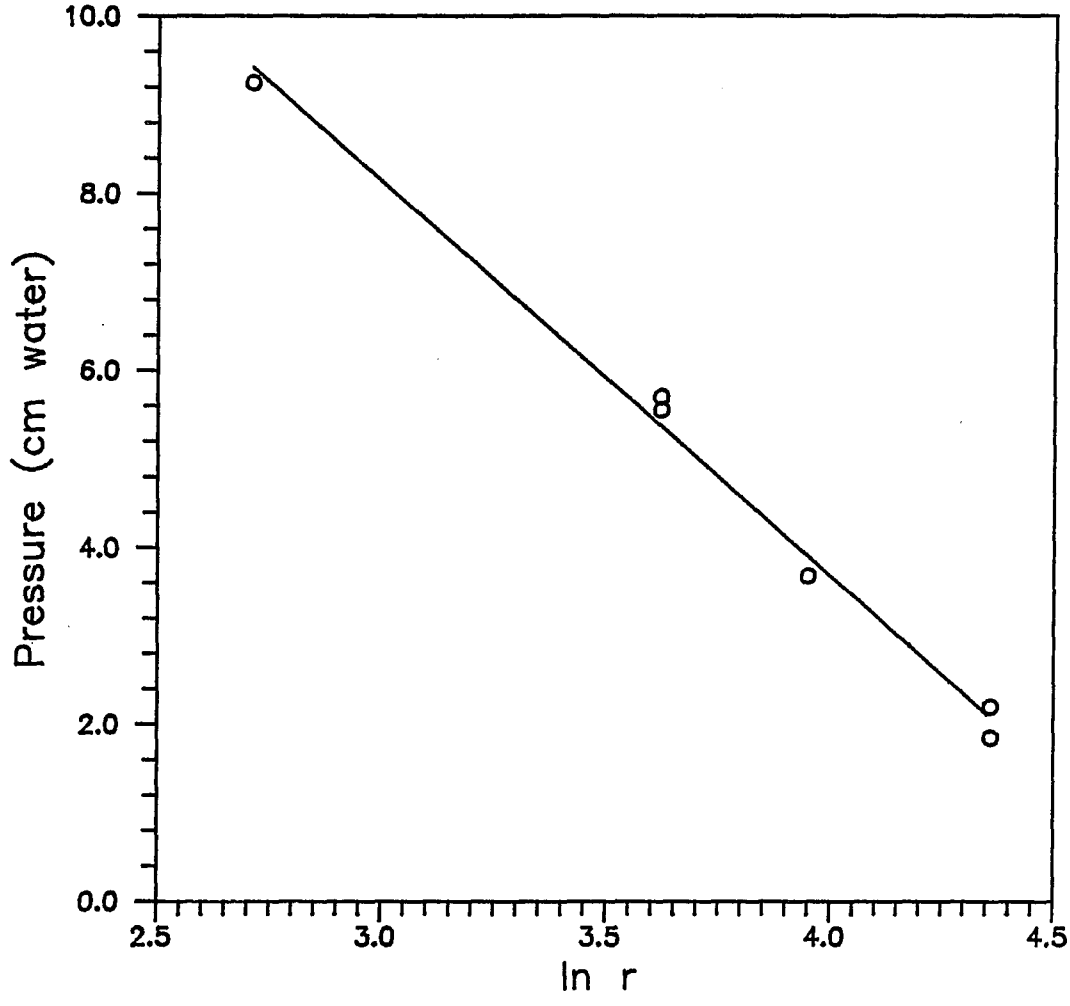

Figure 4.1. Air pressure in soil air pore space was monitored at selected radial distances (r). Plot of air pressure vs. ln r confirmed incompressible radial air flow in the laboratory apparatus.

4.2. HELIUM TRACER TESTS

A mixture of helium (He) and air was used to approximate a conservative vapor phase tracer. Helium was chosen because it is sparingly soluble in water. The solubility of He in water at 25 °C is 0.94 cm^3 He / 100 cm^3 H_2O (CRC). The soil air pore space initially contained no He. The flow from tanks of compressed air and He were mixed and injected into the model. Flow rate was measured continuously with a suspended sphere flow meter which had been calibrated with a soap bubble flow meter. The relative concentration of the tracer was measured with a model 21-150 Gas Leak Detector (Gowmac Instrument Co., Bridgewater, N.J.). The Gas Leak Detector detects the difference in thermal conductivity between air and helium, and was set to read 0 when measuring clean air. He concentration in the injection mixture was increased until a full scale reading was obtained. Input concentration and flow rate were adjusted during the experiment if necessary to keep their values constant. The gas leak detector probe could be positioned to measure from the soil air pore space monitors, individual rear exits, or from the combined effluent. When outflow concentration equalled input concentration, clean air was injected until all He was removed. Concentration data were plotted vs. time to obtain breakthrough curves.

Initial experiments showed breakthrough occurred in the lower advecting layer before breakthrough in the upper layer. It was thought that the disparity was due to either

differences in permeability between the upper and lower advecting layers, or loss of helium by diffusion from the upper layer into the void space at the top of the model. A plastic sheet which sealed the top layer of soil was added to test the diffusion hypothesis. When the tracer experiment was conducted with the plastic sheet in place, congruent breakthrough in each of the advecting layers was observed. Figure 4.2 illustrates breakthrough curves for the upper and lower soil layers. The asymmetry of the breakthrough curve was due to fluctuations in the input concentration. A similar response from the upper and lower layers confirmed that diffusion of He into the void space at the top of the model was responsible for slower breakthrough in the upper layer.

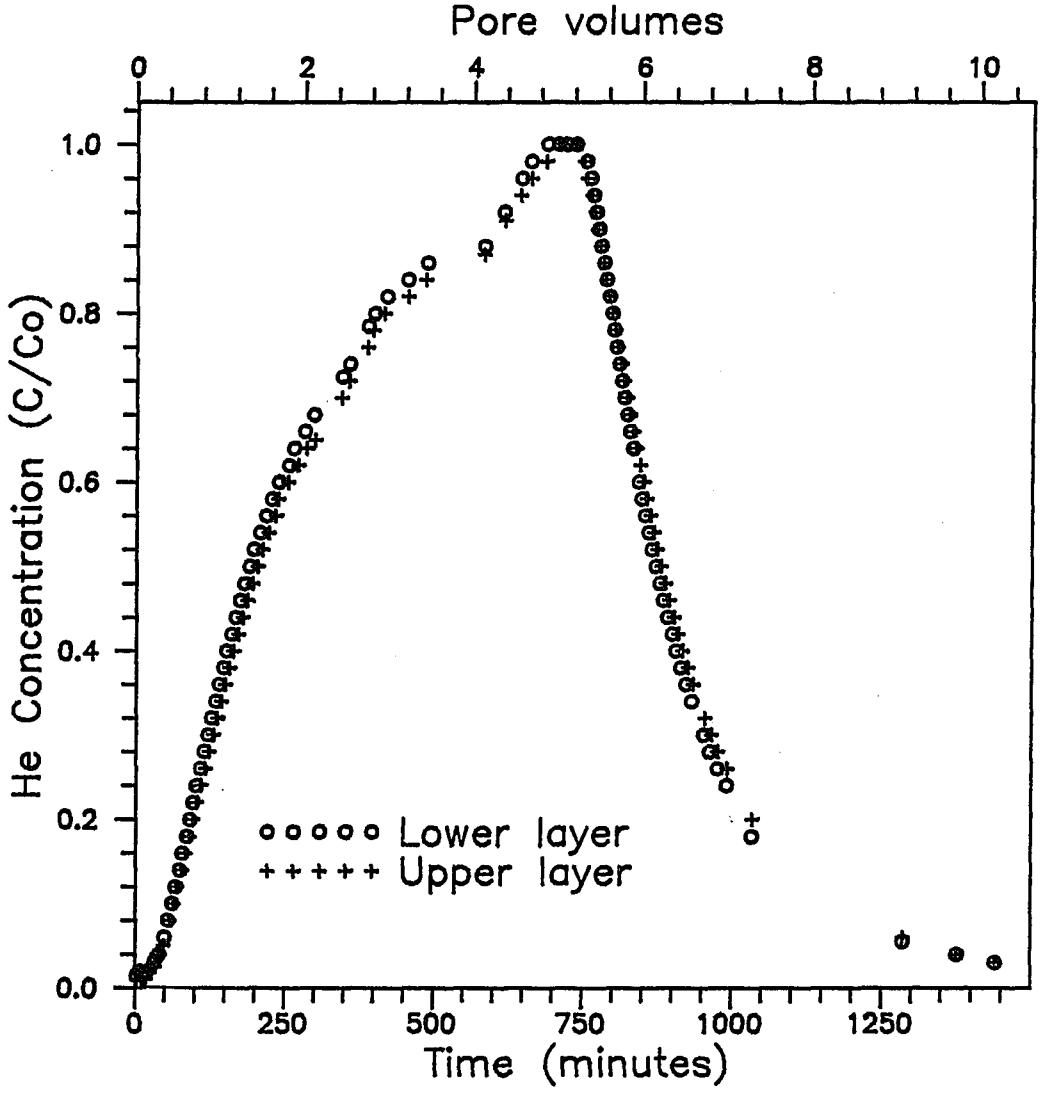

Figure 4.2. Similar flow characteristics of the upper and lower advecting layers are illustrated with He tracer breakthrough curves.

Another experiment was performed, and the input concentration was closely monitored. Outflow of the upper and lower layers were combined since their response was similar, and the averaged concentration was measured. The measured breakthrough curve is presented in Figure 4.3. The observed tailing may be due to diffusion of He between the advecting and confining layers, and dissolution of He into the soil water.

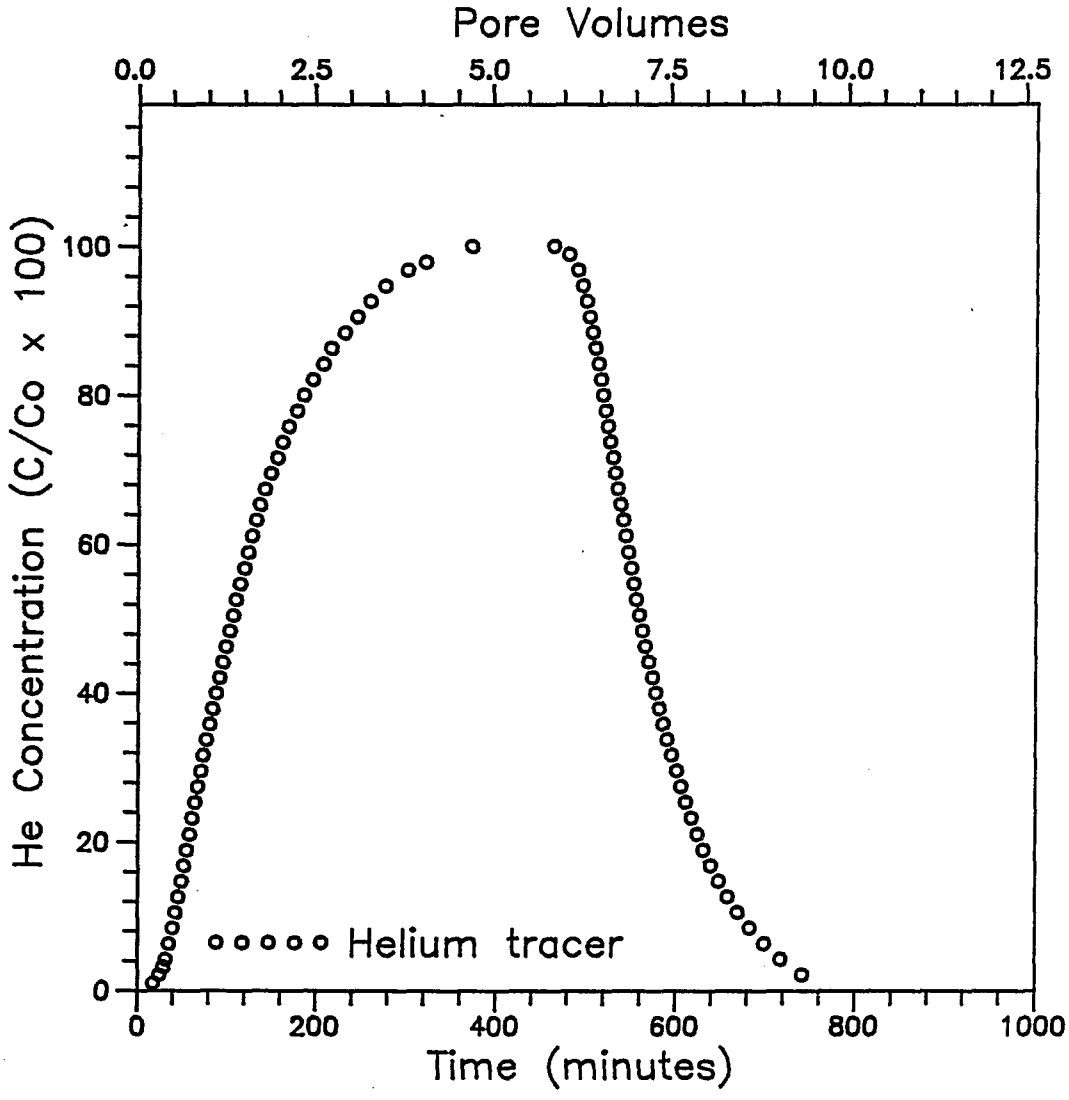

Figure 4.3. Helium tracer breakthrough curve using the average concentration from the upper and lower advecting layers.

4.3. VOC INJECTION AND MEASUREMENT

To introduce TCE into the system, clean air was passed through a gas washing bottle partially filled with liquid TCE. TCE vaporized into the air stream, and was injected into the model. Air flow rate was monitored continuously with a suspended sphere flow meter installed upstream from the gas washing bottle. A constant TCE input concentration was desired, but it was difficult to achieve. When a bubbler was used in the evaporation flask, TCE condensed in the tubing and caused the tubing to lose integrity. Leakage then became a problem. Passing air over the liquid TCE surface did not provide a constant input concentration. However, this method was considered more appropriate, given the health and safety concerns regarding TCE. TCE vapor was injected continuously for 30 days to allow equilibration between the vapor, liquid, and sorbed phases. TCE vapor concentration was monitored until input and exit concentrations were equal. Due to experimental difficulties, the input portion of the TCE breakthrough curve was not recorded.

The vapor phase concentration of 1,1,1-TCA was also monitored. It had been in the system for several months due to use of the Locktite adhesive during construction, and was assumed to have partitioned with the liquid and solid phases.

4.3.1. VOC ANALYSIS

Analysis of TCE and 1,1,1-TCA was accomplished with a

Varian 3300 gas chromatograph with an electron capture detector (ECD), and a Varian 4290 integrator. A 6 foot column with 1% SP-1000 on 60/80 carbopack was used. Similar column retention times of 1,1,1-TCA and TCE coupled with increased sensitivity of the electron capture detector for 1,1,1-TCA caused masking of the TCE peak early in the experiment. During the first days of the experiment, it was necessary to program the column temperature to separate the 1,1,1-TCA peak from the TCE peak. The initial column temperature was 50 °C with a 1 °C min^{-1} rate increase to 80 °C; hold for 3 minutes; temperature increase of 20 °C for 2 minutes to 120 °C, and hold for 10 minutes.

During the TCE injection phase, 1,1,1-TCA was being stripped from the system, and this outflow concentration was reduced. After several days of ventilation, the 1,1,1-TCA peak no longer masked the TCE peak, and the column temperature was set to operate isothermally at 150 °C. The injector and detector temperatures remained constant at 175 °C, and 200 °C respectively.

Experiments were conducted which determined that the ECD had a linear response over the range of concentrations encountered in this investigation. Calibration standards were prepared by injecting measured quantities of liquid TCE or 1,1,1-TCA into 9 ml glass vials sealed with a teflon septa and a screw top. Calibration samples were allowed to volatilize for 45 minutes before injection by gastight syringe into the

gas chromatograph. The gas chromatograph was calibrated at least once for every 50 samples.

4.4 VOC EXTRACTION

After the vapor injection period, clean air was introduced into the laboratory model. Forced ventilation was run continuously for 47 days, and the effluent vapor concentration of TCE and 1,1,1-TCA were monitored with time. Clean air injection was varied from 140 to 700 ml/min to determine the effect of flow rate on vapor concentration. A correlation was observed between flow rate and outflow vapor concentration. Effluent vapor concentration increased when a relatively low air flow rate followed a high rate of flow. Since the liquid and vapor phases were determined to be near equilibrium (Section 4.5), VOC desorption from the solid phase is thought to have produced the increase in vapor concentration. When air flow rate was increased, vapor concentration dropped to a lower level. The relationship between flow rate and vapor concentration was illustrated in the air stripping record.

The TCE data are presented in Figure 4.4, and the 1,1,1-TCA data are shown in Figure 4.5. Scatter in TCE data collected between 0 and 100 pore volumes may have been due to sampling with a syringe without a gastight tip. The data collected during the extraction phase were not adversely affected by the presence of 1,1,1-TCA except at lower TCE

concentrations where masking, again, became a problem. The reason for the discontinuity in the TCE data trend at about 200 pore volumes is not clear. Concentration rise immediately following the discontinuity is due to a decrease in volumetric flow rate. Volumetric flow rates are indicated below the graphs.

To determine the VOC concentration in the aqueous phase, 8 ml aqueous samples were withdrawn from the bottom suction candles, injected into a 9 ml vial, capped and allowed to equilibrate up to 24 hours. The vapor in the bottle headspace was then sampled and analyzed with the gas chromatograph. Vapor concentration of 1,1,1-TCA in the headspace of aqueous samples closely matched the effluent vapor concentration of the laboratory apparatus.

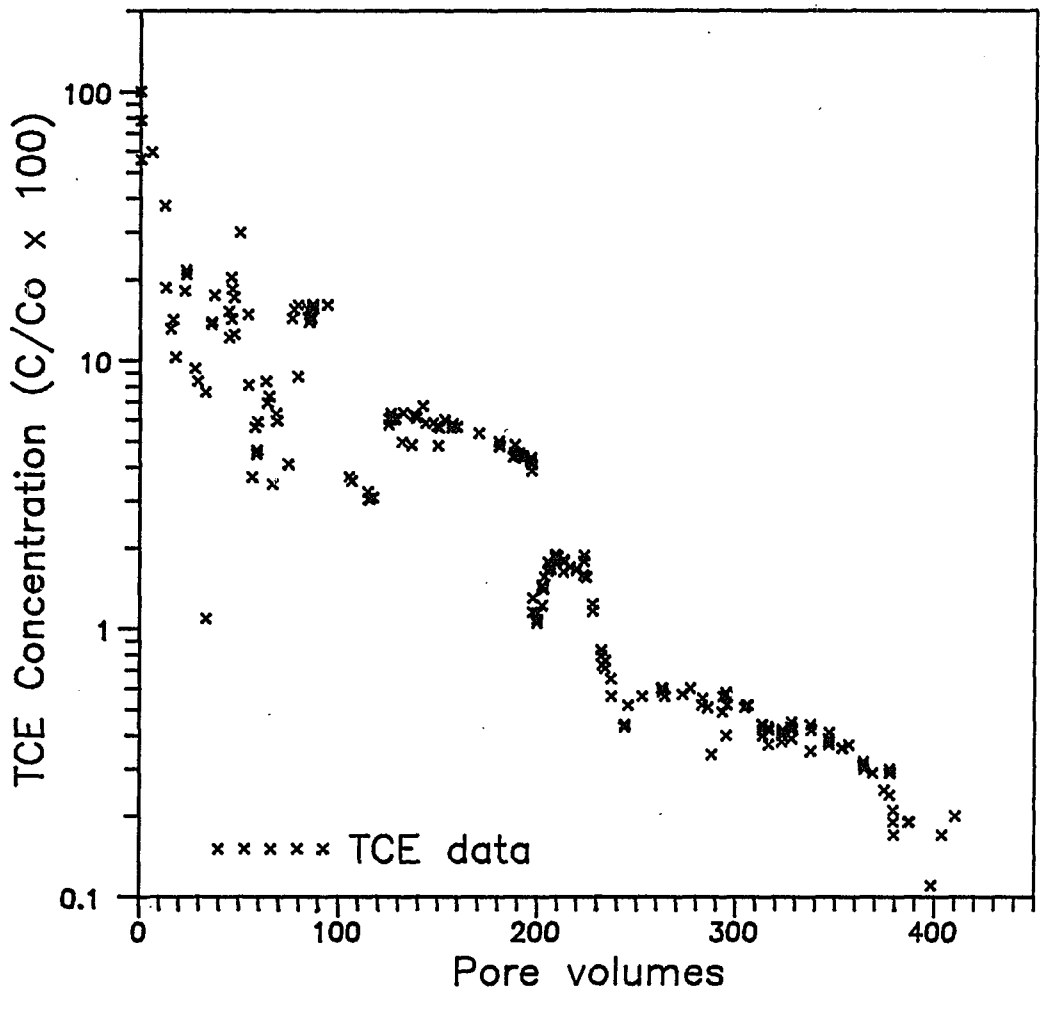

Pore Volumes	Flow (ml/min)	Pore Volumes	Flow (ml/min)
0.0 - 3.6	148	197.8 - 199.5	400
3.6 - 124.5	400	199.5 - 201.1	250
124.5 - 128.7	140	201.1 - 224.0	140
128.7 - 188.5	400	224.0 - 382.1	400
188.5 - 194.1	348	382.1 - 384.0	700
194.1 - 196.9	285	384.0 - 391.4	400
196.9 - 197.8	250	391.4 - 410.4	700

Figure 4.4. TCE air stripping record for 47 days. Note that vapor concentration increases when air flow rate is decreased.

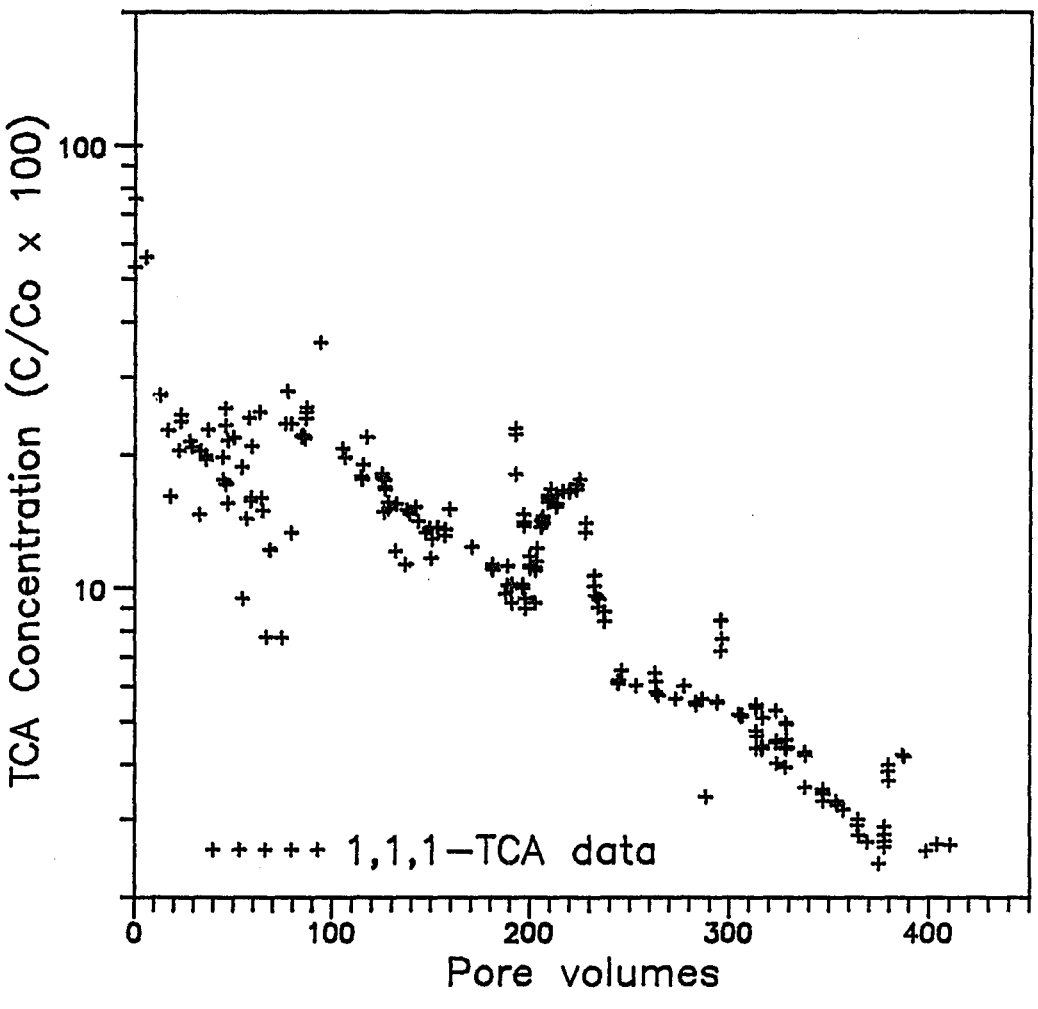

Pore Volumes	Flow (ml/min)	Pore Volumes	Flow (ml/min)
0.0 - 3.6	148	197.8 - 199.5	400
3.6 - 124.5	400	199.5 - 201.1	250
124.5 - 128.7	140	201.1 - 224.0	140
128.7 - 188.5	400	224.0 - 382.1	400
188.5 - 194.1	348	382.1 - 384.0	700
194.1 - 196.9	285	384.0 - 391.4	400
196.9 - 197.8	250	391.4 - 410.4	700

Figure 4.5. 1,1,1-TCA air stripping record for 47 days.

The amount of TCE removed during 47 day experiment was estimated by plotting vapor phase concentration (mg/l) vs. pore volumes (1 pore volume = 56.5 l). An exponential trend was observed (see Figure 4.6) and the equation of a best fit line was determined to be $Y = 11.731(e^{-.0126X})$. The solution to the equation integrated between 0 and 410 pore volumes is 52.3 grams TCE. Sample calculations are shown to compare the amount of mass expected to be in each phase given the estimated amount of TCE removed. The measured vapor concentration of TCE at the onset of air stripping was 46.7 mg/l. Total volume calculations of air, water and soil assume the model outline to be an equilateral triangle with sides of 100 cm, and a base of 86.6 cm. Total height of the advecting layers was 48 cm, and 20 cm for the confining layers. Porosities and degree of saturation values obtained from core samples (Table 3.1) were used for both soils. Total air volume was calculated to be 69.6 liters. 3.25 grams of TCE were estimated to exist in the vapor phase by:

$$TCE_v = (C_{ao})(V_a) \qquad (4.1)$$

where TCE_v = total TCE in vapor phase (mg)

C_{ao} = initial vapor concentration (mg/cm^3)

V_a = total air volume (cm^3)

The total volume of liquid in the laboratory model was

52.4 liters. 7.94 grams of TCE were estimated to be in the dissolved phase by:

$$TCE_l = (C_{ao}/H_c)(V_l) \qquad (4.2)$$

where TCE_l = total TCE in liquid phase (mg)

V_l = total liquid volume (cm^3)

The mass of soil was estimated using bulk density values obtained from core samples and the soil volume calculations mentioned earlier. The total soil mass calculated was 458,633 grams. The total soil mass was used because the fraction organic carbon was the same for both soils. 11.47 grams TCE in the solid phase was then calculated by:

$$TCE_s = (M_s)(K_p C_l) \qquad (4.3)$$

where TCE_s = total TCE in sorbed phase (mg/g)

M_s = mass of soil (g)

The total mass estimated for all phases was 22.66 grams. Assuming that the estimate of Kp is accurate, 29.6 grams of TCE could have desorbed from the adhesive and/or plexiglass walls of the laboratory apparatus.

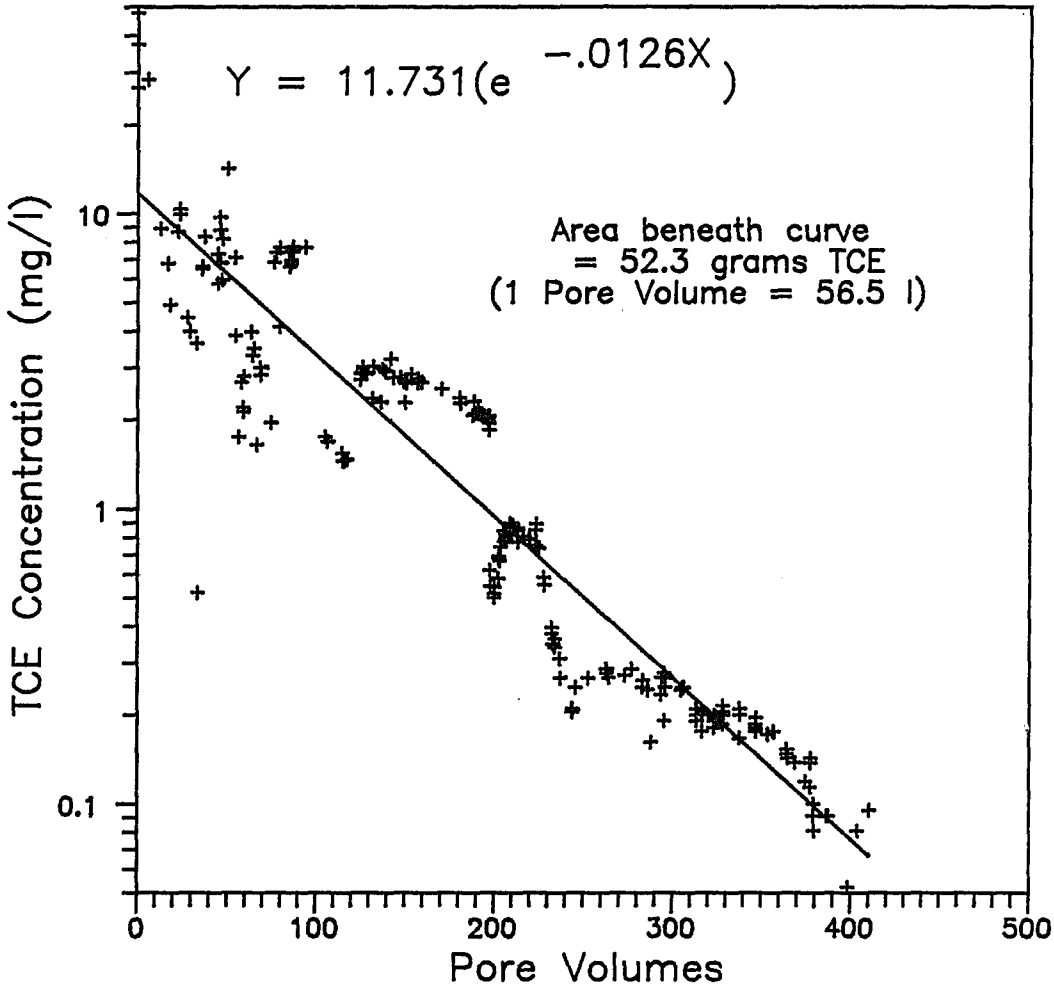

Figure 4.6. TCE vapor concentration data display an exponential decay. Integrating to find the area beneath the curve indicate that 52.3 grams of TCE was removed.

4.5 LIQUID - VAPOR MASS TRANSFER MEASUREMENTS

To measure the liquid - vapor mass transfer rate, 3 ml of solution drawn from the bottom set of suction lysimeters was injected into each vial and sealed. The vapor accumulating in the headspace was analyzed with the gas chromatograph. The resulting equilibrium vapor concentration in the headspace was consistently 30 to 40 percent lower than the observed vapor concentration in the model. To determine if mass transfer from the liquid to vapor was significantly lowering the aqueous concentration, batch experiments were conducted with 8 ml of solution and 1 ml headspace. The vial was capped as before and vapor samples were withdrawn with a gastight syringe. The sample bottle was inverted between sampling so that liquid contacted the septa after it had been punctured. This prevented loss of VOC sample through the septa holes. Measurements were made over a 1 hour period, and the concentration values were plotted against time. Mass transfer from liquid to vapor occurred in the vials for 35 to 40 minutes before equilibrium was established. Figure 4.6 illustrates the liquid - vapor mass transfer rate measured with the batch experiments.

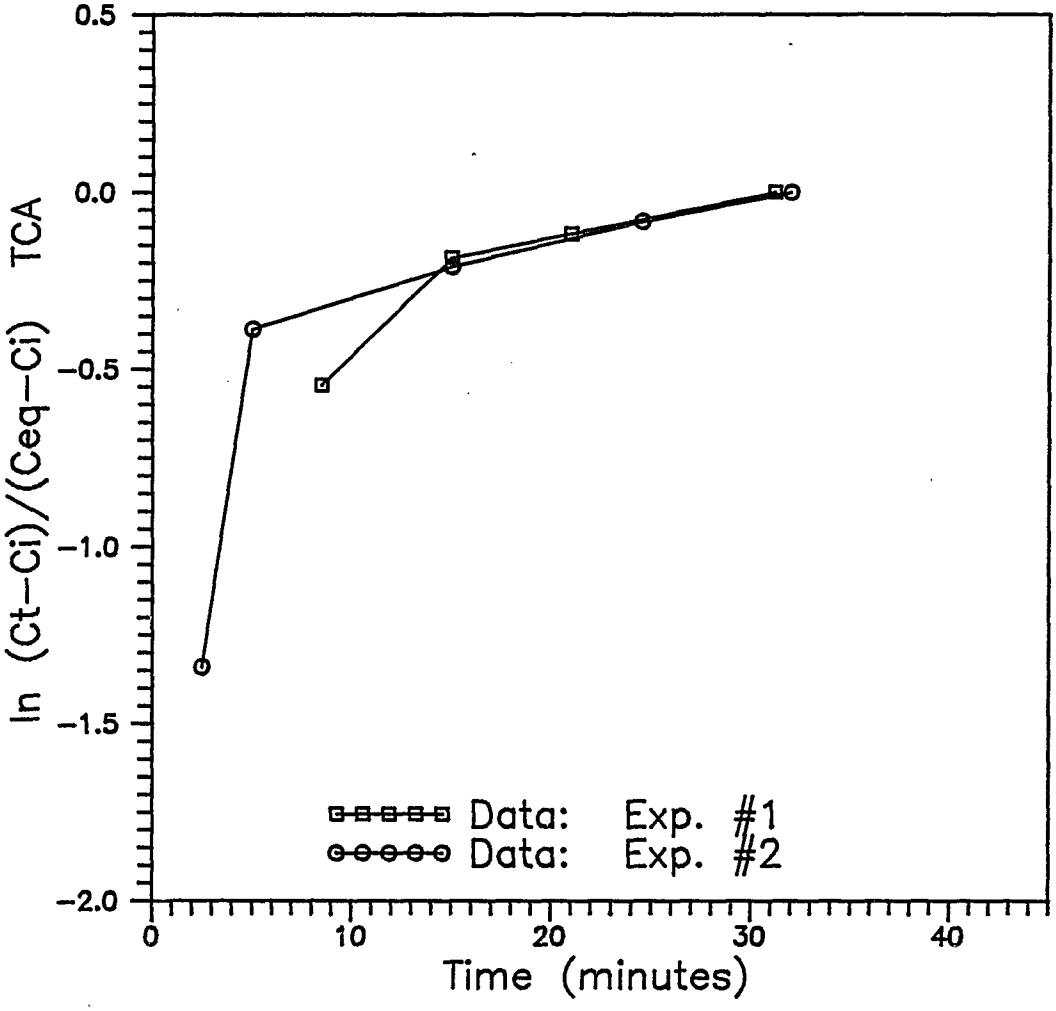

Figure 4.6. Graph of liquid - vapor mass transfer for 1,1,1-TCA measured in batch experiments

The flow rates used in the experiment were between 140 and 700 ml/min. The total volume of air pore space in the advecting layers was 56.5 l. The calculated residence time of injected air had a range of 80 - 400 minutes. This indicated that near equilibrium conditions between dissolved phase and vapor existed in the laboratory model. Additionally, the headspace vapor concentration obtained from batch experiments using 8 ml of liquid corresponded well with the effluent vapor concentration measured in the model. Based on these data, near equilibrium conditions were assumed between liquid and vapor phases in the laboratory model.

The mass transfer from liquid to vapor is dependent on the exposed surface area at the liquid - vapor interface, and from diffusional resistance in the liquid. The liquid -vapor interface in unsaturated soil is probably much larger than in the batch experiments. However, the batch experiments provided an approximate mass transfer rate, and helped confirm near equilibrium conditions between liquid and vapor.

The only compound detected in the vial headspace was 1,1,1-TCA. Lack of TCE detection may have been due to masking by the 1,1,1-TCA peak. Since the physical and chemical properties of TCE and 1,1,1-TCA are similar, the liquid - vapor mass transfer rate measured for 1,1,1-TCA was also used for TCE in the computer simulation.

4.6 SOLID - LIQUID - VAPOR MASS TRANSFER MEASUREMENTS

The solid - liquid - vapor mass transfer rate was obtained by measuring the re-equilibration of soil vapor after more than 50 days of air stripping. After a period of air stripping, the vapor phase was not in equilibrium with the solid phase. The increase in vapor phase concentration that resulted from mass transfer from the solid phase was measured over a period of 20 days. Initial vapor concentration of TCE was 100 µg/l TCE, and 0.1 µg/l for 1,1,1-TCA. Clean air was injected for 10 minutes to obtain a vapor sample, and then turned off. The experimental method assumes that the small amount of clean air introduced in the model to facilitate sampling has a negligible effect on mass transfer within the solid - liquid - vapor system. Figure 4.7 illustrates the results of the experiment.

Vapor samples taken over a period of 20 days indicate an initial fast desorption rate for about 5 days followed by a slower rate. One explanation for the two rates is that the initial step reflects VOC desorption near the surface of the organic matter, and the slower step was due to VOC diffusion through organic matter and soil aggregates. Another explanation is that the adhesive on the walls of the laboratory apparatus could be responsible for fast VOC desorption, and the slow step due to desorption/diffusion from the organic matter and soil aggregates.

The measured desorption rate from solid to liquid to

vapor is nearly 3 orders of magnitude slower than the measured rate for desorption from liquid to vapor. The results suggest that mass transfer from the solid to the liquid phase may be a slow process. In this case, however, it is impossible to separate out the effects of the adhesive and plexiglass on the rates of desorption.

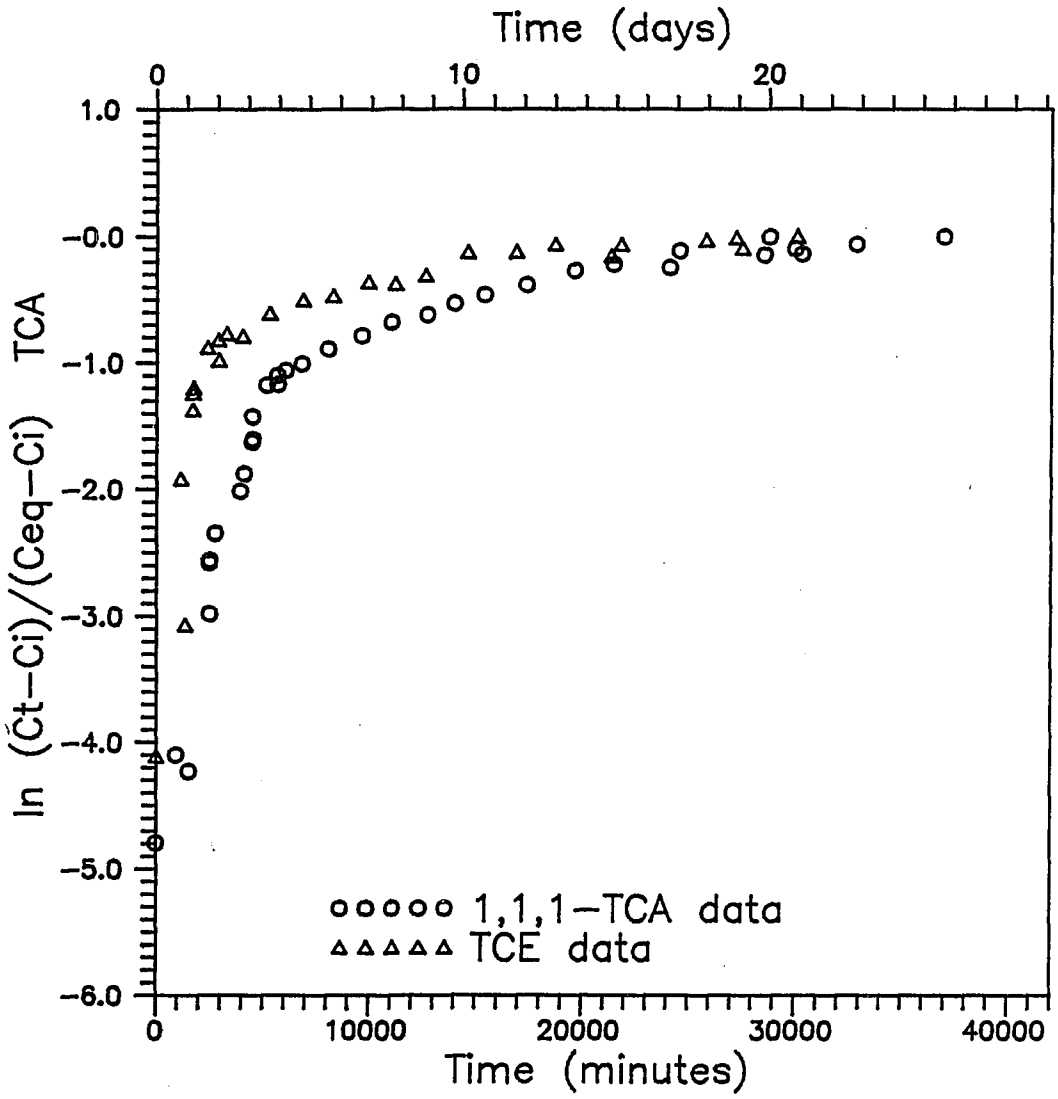

Figure 4.7. Rate of vapor accumulation that resulted in the laboratory apparatus after forced ventilation was halted.

5. NUMERICAL MODELING

5.1 INTRODUCTION

A numerical mixing cell model was used to simulate clean air flow through unsaturated, layered soil containing TCE and 1,1,1-TCA. Initially, equilibrium partitioning was assumed between the solid, liquid, and vapor phases. A film of water was assumed to cover each soil grain, and allowed mass transfer to occur from solid to liquid, and from liquid to vapor. As clean air was injected, mass transfer from liquid to vapor occurred in response to the lowering vapor concentration. As the aqueous phase concentration was reduced, mass transfer from the solid phase to liquid occurred. Since advection in the confining layer was minimal, diffusion was modeled between the confining layer, and the advecting layer.

The Discrete State Compartment model (DSC) has been used by Rasmussen (1982) to model solute transport through dual porosity media. Roberts (1987) used The DSC model to predict the movement of volatile fluorocarbons in the unsaturated zone. Seidemann (1988) also simulated vapor transport in the unsaturated zone.

A copy of the DSC User Manual is included in Appendix A. It presents an overview of the mathematical relationships

employed by the model, and a description of program input parameters.

5.1.1 MODEL DESCRIPTION

The DSC model uses two algorithms to simulate mass transfer. The simple mixing cell algorithm moves a volume from the first compartment and mixes it with the second. After mixing in the second compartment, an equivalent volume is transferred back to the first compartment. In the modified mixing cell algorithm, a volume of the first cell is displaced by an incoming volume. The displaced volume mixes with the second cell, and the incoming volume mixes with the remaining cell contents. Exchange parameters are unique to the algorithm being used.

In the advection scheme, the parameter is called the boundary recharge volume (BRV). It is found by:

$$BRV = Q\ dt / Vol\ 1 \qquad (5.1)$$

where Q = volumetric flow rate ($cm^3\ min^{-1}$)

dt = time for 1 iteration (min)

$Vol\ 1$ = volume of cell 1 air porosity (cm^3)

The boundary recharge concentration (BRC) is the parameter that sets the incoming concentration.

The Ri parameter is used in the simple mixing cell

algorithm to set the exchange volume. Numerically, it is the volume percentage of the first cell that is transferred to the second. The DSC Users Manual (Appendix A) defines the Ri coefficient as:

$$Ri = Vol_2\ D\ A\ n_2\ dt/(Vol_1\ (Vol_2\ dx - D\ A\ n_1\ dt)\ ) \qquad (5.2)$$

where Vol_2 = volume of cell 2 (cm^3)

Vol_1 = volume of cell 1 (cm^3)

D = coefficient of diffusion ($cm^2\ s^{-1}$)

A = cross sectional area (cm^2)

n_2 = cell 2 air filled porosity (cm^3 air cm^{-3} porous media)

n_1 = cell 1 air filled porosity (cm^3 air cm^{-3} porous media)

dx = linear diffusive path (cm)

dt = time increment (s)

The calculated Ri is highly dependent on x, and therefore the soil air tortuosity. The diffusion coefficient used in the calculation was determined by Westenberg and Walker (1957) for He to N_2 as 0.705 $cm^2\ s^{-1}$ The DSC model is intended to solve the advection-dispersion equation (2.17) by separating it into separate advection and diffusion components. The advection scheme is appropriate when vapor movement from one compartment to another is driven by a

pressure gradient. The diffusion scheme is appropriate when movement occurs in response to a concentration gradient.

In this investigation, the modified mixing cell algorithm was used to simulate advection of air through the soil air pore space, and the simple mixing cell was used to represent diffusion. The simple mixing cell was also used to simulate mass transfer between solid, liquid, and vapor phases. Figure 5.1 illustrates the modified mixing cell, and the simple mixing cell algorithms.

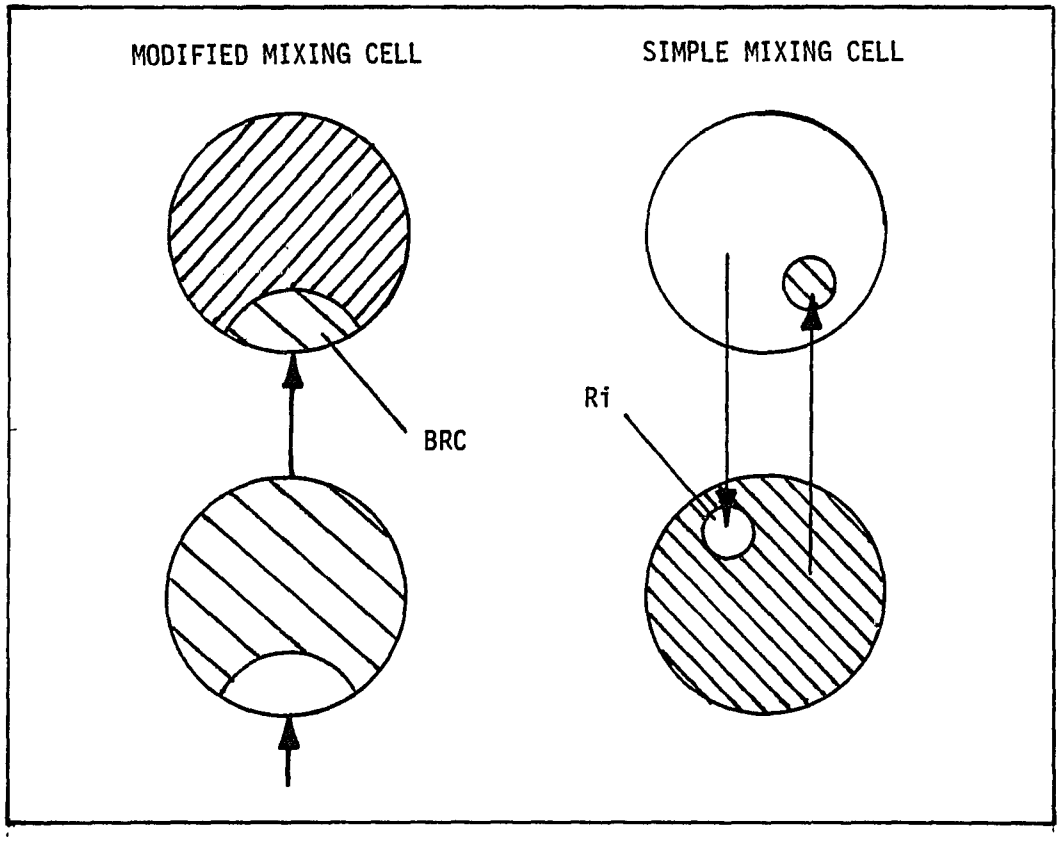

Figure 5.1. The exchange parameters are illustrated for the modified mixing cell and simple mixing cell algorithms.

5.2. CONSERVATIVE TRACER SIMULATION

To simulate radial flow, the relative volumes of the compartments were enlarged with incremental increase in radial distance. The relationship is shown by integrating with respect to r:

$$2\pi h \int r dr = \pi h(r^2_2 - r^2_1) \qquad (5.3)$$

where h = height of compartment

r = radial distance

The first compartment in the model was assigned a volume of 1, and others increased by steps to 3, 5, 7, 9, and etc. The upper boundary was set at the midpoint of the bottom confining layer. This allowed for diffusion into the confining layer from both upper and lower advecting layers, but only the lower half of the confining layer and the bottom advecting layer was considered in the modeling. The lower boundary was assumed to be impermeable (the plexiglass bottom). A schematic of the modeled geometry is illustrated in Figure 5.2

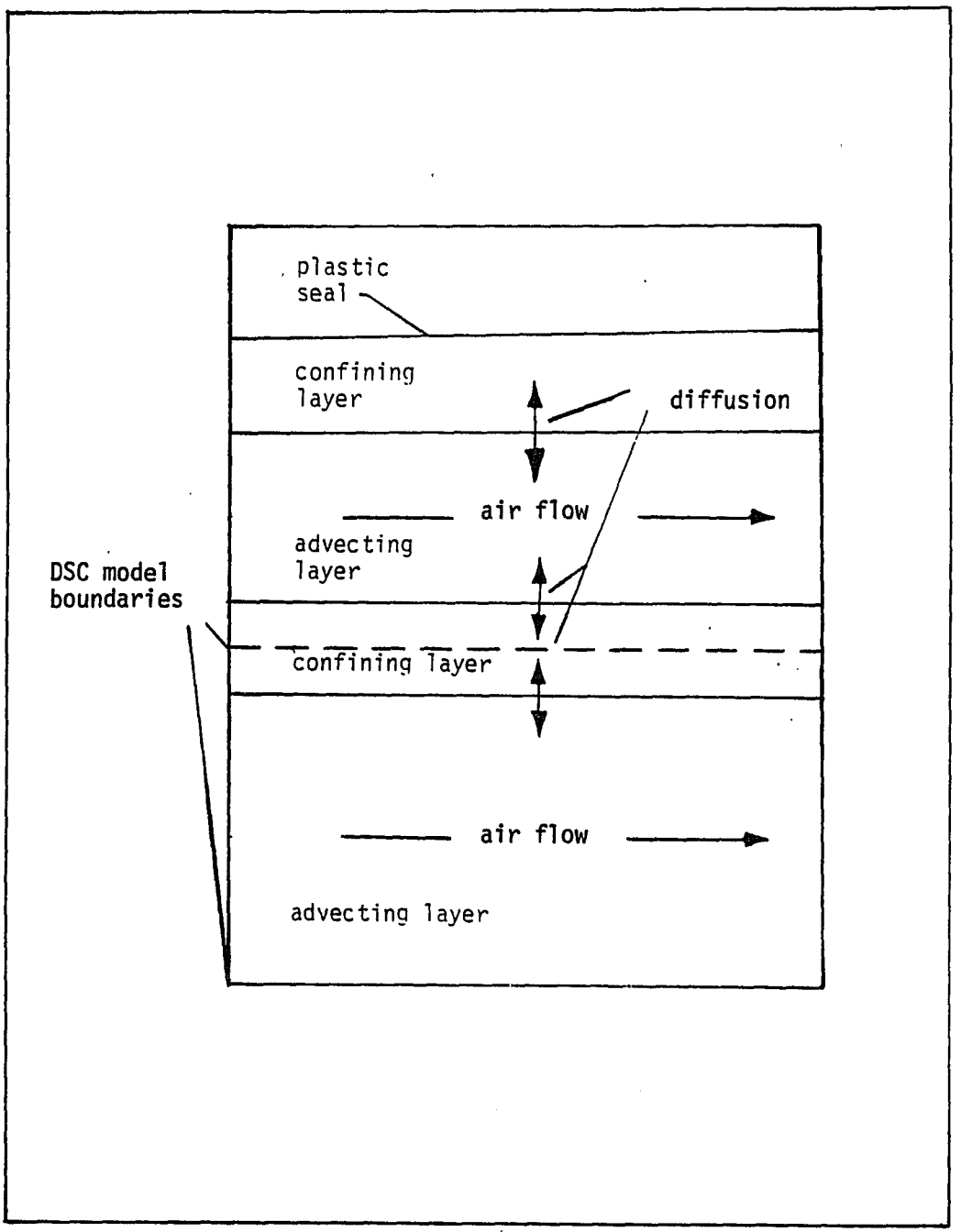

Figure 5.2. For modeling purposes the upper boundary was set at the midpoint of the bottom confining layer.

During the injection phase of the helium tracer experiment, the confining layer was treated as a sink term. A concentration gradient developed between the confining and advecting layers, and the helium - air mixture diffused from the advecting layer to the confining layer. After breakthrough occurred, the confining layer acted as a source, and the diffusion path was reversed. Figure 5.3 depicts the cell geometries and the mass transfer algorithms between them.

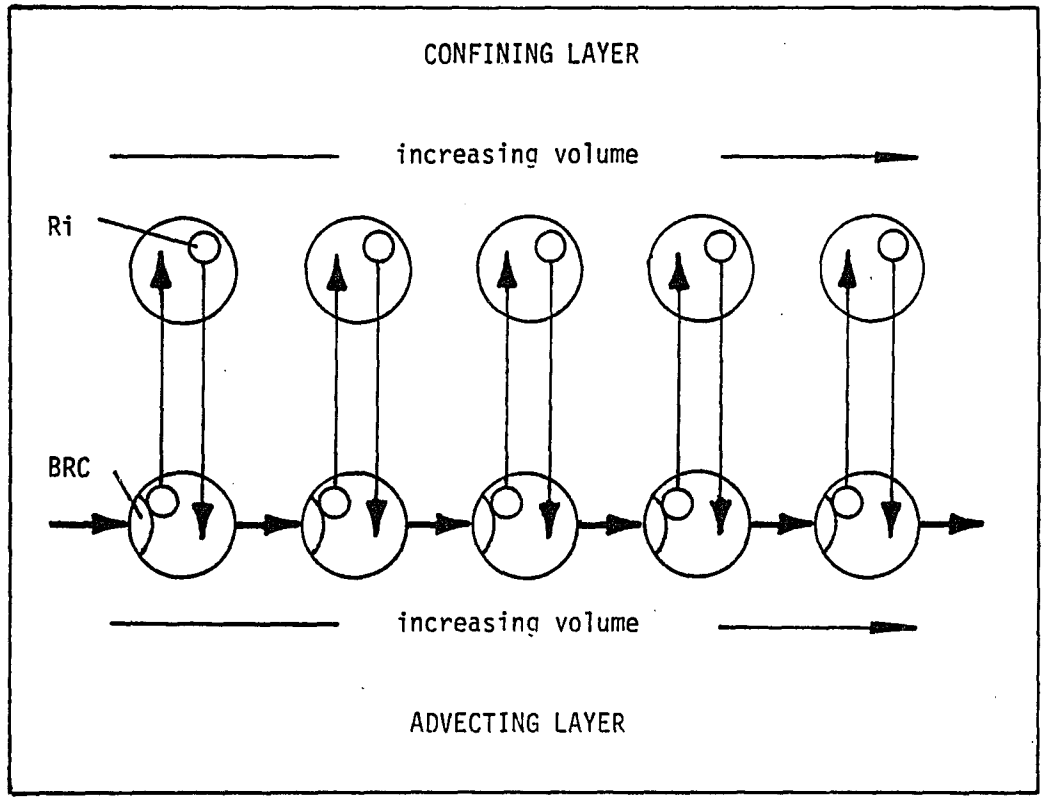

Figure 5.3. Cell geometry used to simulate movement of a conservative tracer in radial coordinates.

The DSC model was used to simulate conservative tracer flow in the model. For modeling purposes it was assumed that the soil extended to the apex of the lysimeter (i.e. the gravel pack was neglected). Diffusion between the advecting and confining layer was modeled with the simple mixing cell algorithm. The confining layer acted as a sink during tracer injection, and a He source during clean air injection. The Ri parameter was calculated using Equation 5.2 and adjusted until the simulated breakthrough curve most closely matched the measured curve. Dissolution of He into soil water was not accounted for. Figure 5.4 compares the model simulation of a conservative tracer to the measured He breakthrough curve.

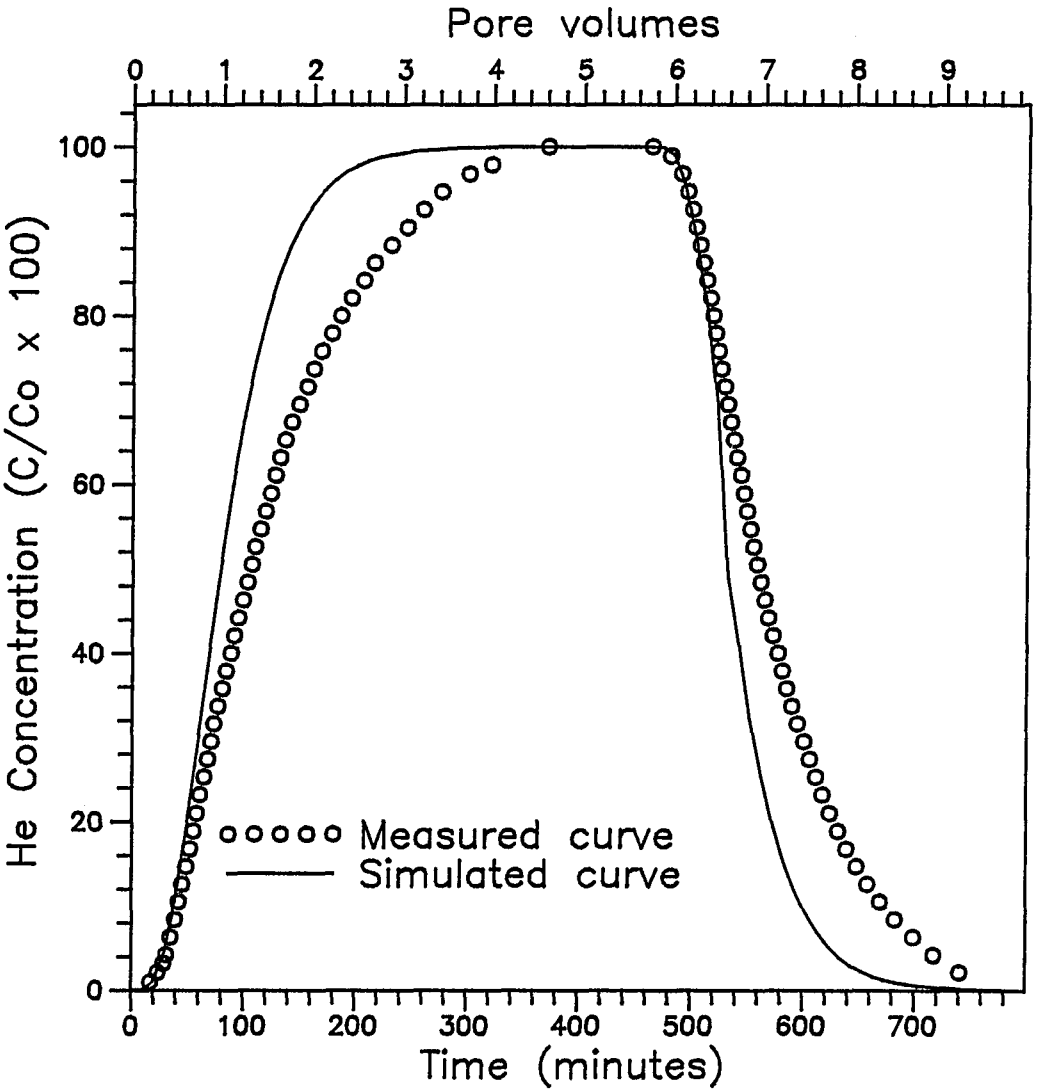

Figure 5.4. Conservative tracer breakthrough curve simulated with DSC model is compared to measured breakthrough curve using a helium tracer.

5.3 MASS TRANSFER: LIQUID - VAPOR

To simulate VOC mass transfer between the dissolved and vapor phases observed in the batch experiments, a two cell system was employed. The two cell model transferred mass from the liquid cell to the vapor cell in response to a concentration gradient. The initial concentration in the vapor cell was set to zero to reflect the vapor concentration in the glass vial at the onset of the experiment. Liquid concentration was calculated using the vapor concentration and Henry's constant.

The ratio of vapor to dissolved concentration is equal to the Henry's constant at equilibrium in the real system, but in the DSC model, equivalent concentrations define equilibrium conditions. A mass balance approach was used to modify the DSC model for VOC mass transfer between phases. To represent the VOC partitioning, the liquid and vapor cell volumes were adjusted so their volume ratio equaled the Henry's constant. Figure 5.5 is a schematic representation of mass transfer between liquid and vapor.

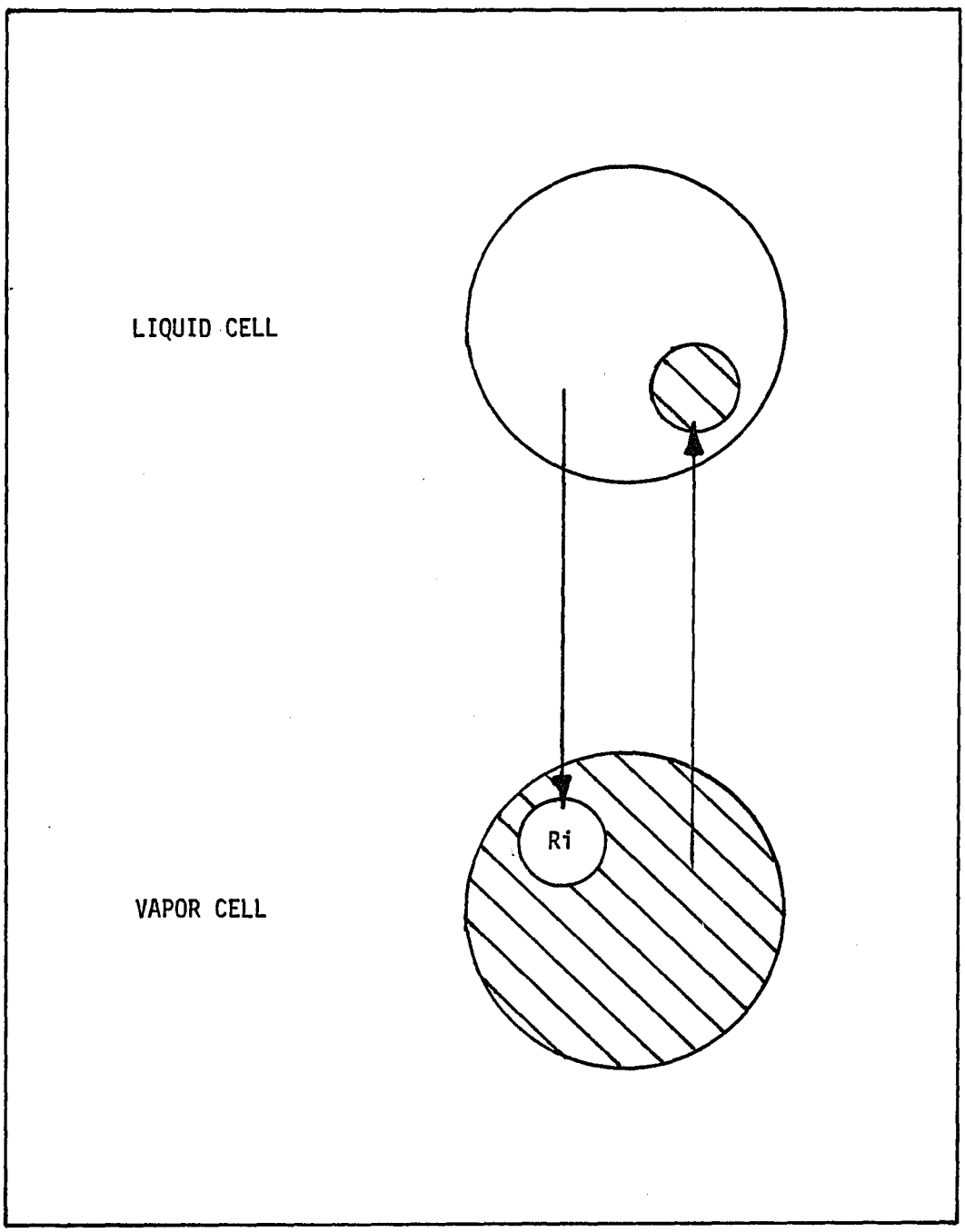

Figure 5.5. Two cell system used to simulate liquid - vapor mass transfer in the DSC model.

The Ri parameter was fitted until simulated mass transfer approximated the experimental data. Because experimental difficulties precluded measurement of TCE in the vial headspace, desorption rates for 1,1,1-TCA were used as approximations for TCE desorption in the computer model. This assumption is reasonable given TCE and 1,1,1-TCA have similar solubilities, octanol-water partition coefficients, and molecular weights. Figure 5.6 illustrates the experimental data, and compares it to simulated desorption with Ri = 0.04.

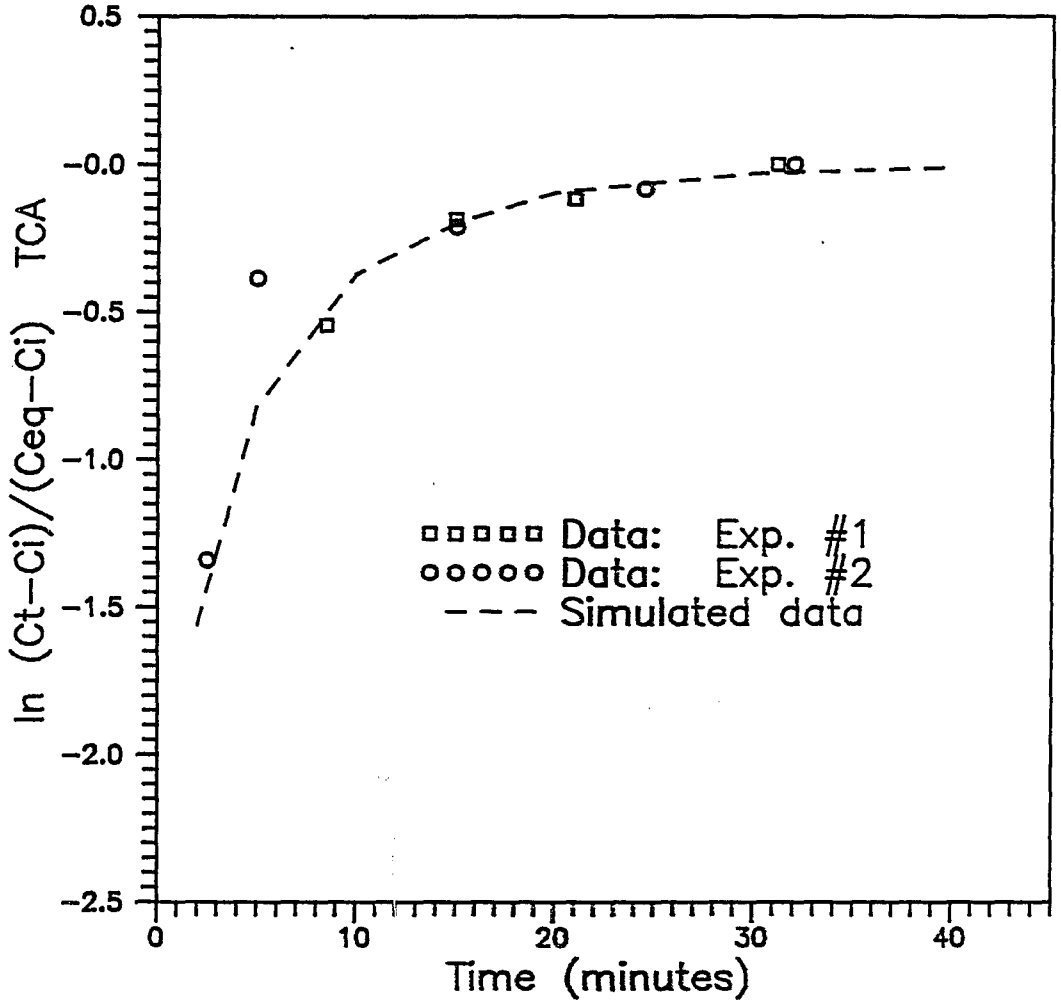

Figure 5.6. The liquid - vapor mass transfer rate measured in batch experiments is compared to DSC model simulated rate.

5.4. MASS TRANSFER: SOLID - LIQUID - VAPOR

To simulate mass transfer between the solid, liquid, and vapor phases, a four cell model was constructed. Liquid and vapor occupied one cell each. The solid phase was divided into two cells with a ratio of 10:1. This arrangement was intended to simulate "fast" VOC desorption near the solid - liquid interface, and slower desorption controlled by diffusion through the organic matter or soil aggregates. The relative cell volumes of the cells were calculated by multiplying the relative fraction of VOC in the soil as calculated with Equation 2.7. The Ri parameter determined previously for transfer between liquid and vapor was used in this model. Ri parameters were fitted to the data to determine the values for diffusion through the solid, and desorption to the liquid which most closely matched the experimental data. Figure 5.7 is a schematic representation of mass transfer between the solid, liquid, and vapor phases.

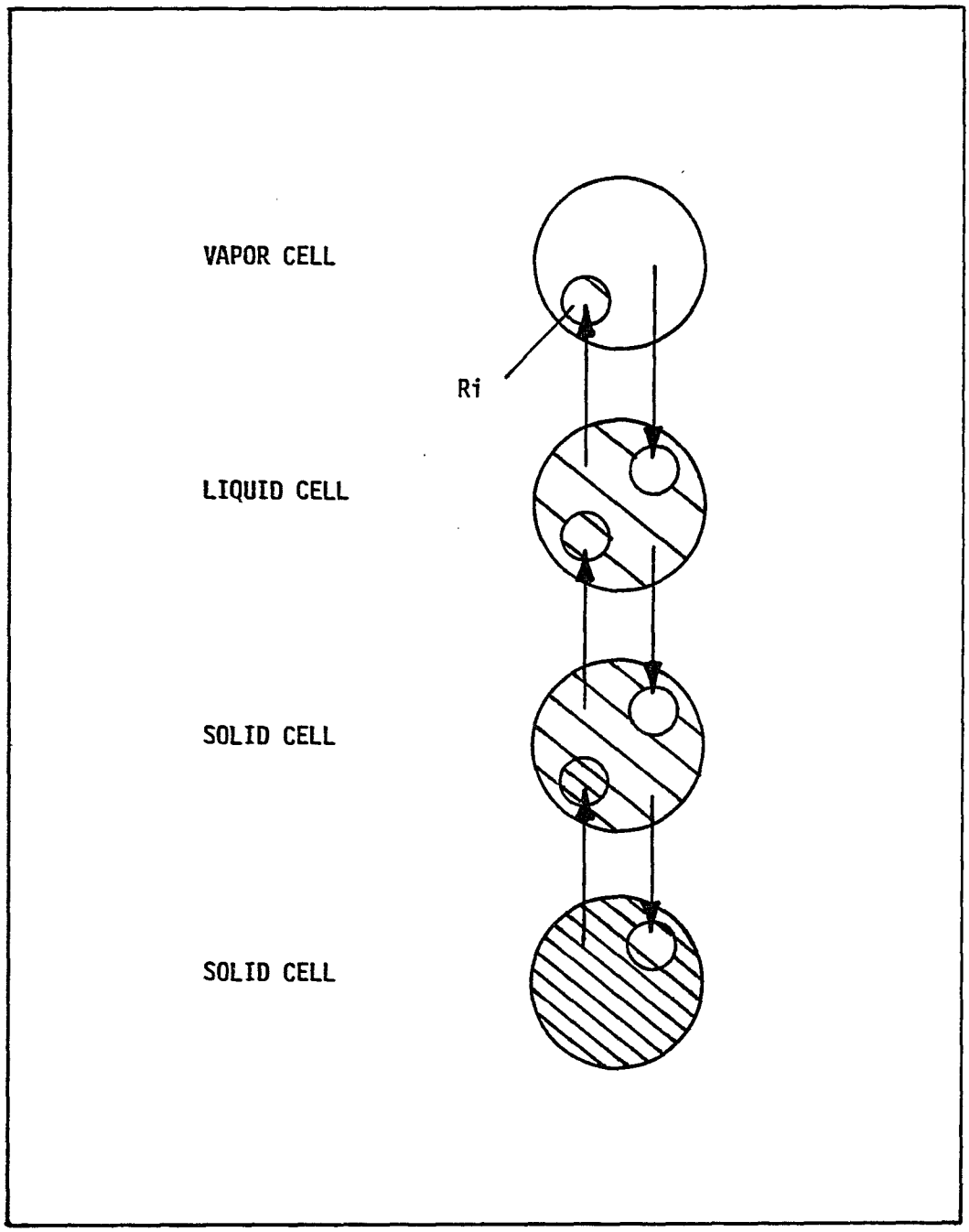

Figure 5.7. Schematic representation of mass transfer between the solid, liquid and vapor phases.

The curve fitting exercise resulted in two Ri values, one responsible for rapid mass transfer at the surface, and the other responsible for slower mass transfer. The Ri parameter determined previously for liquid - vapor desorption was used in this model. Figure 5.8 compares the experimental data to the simulated data.

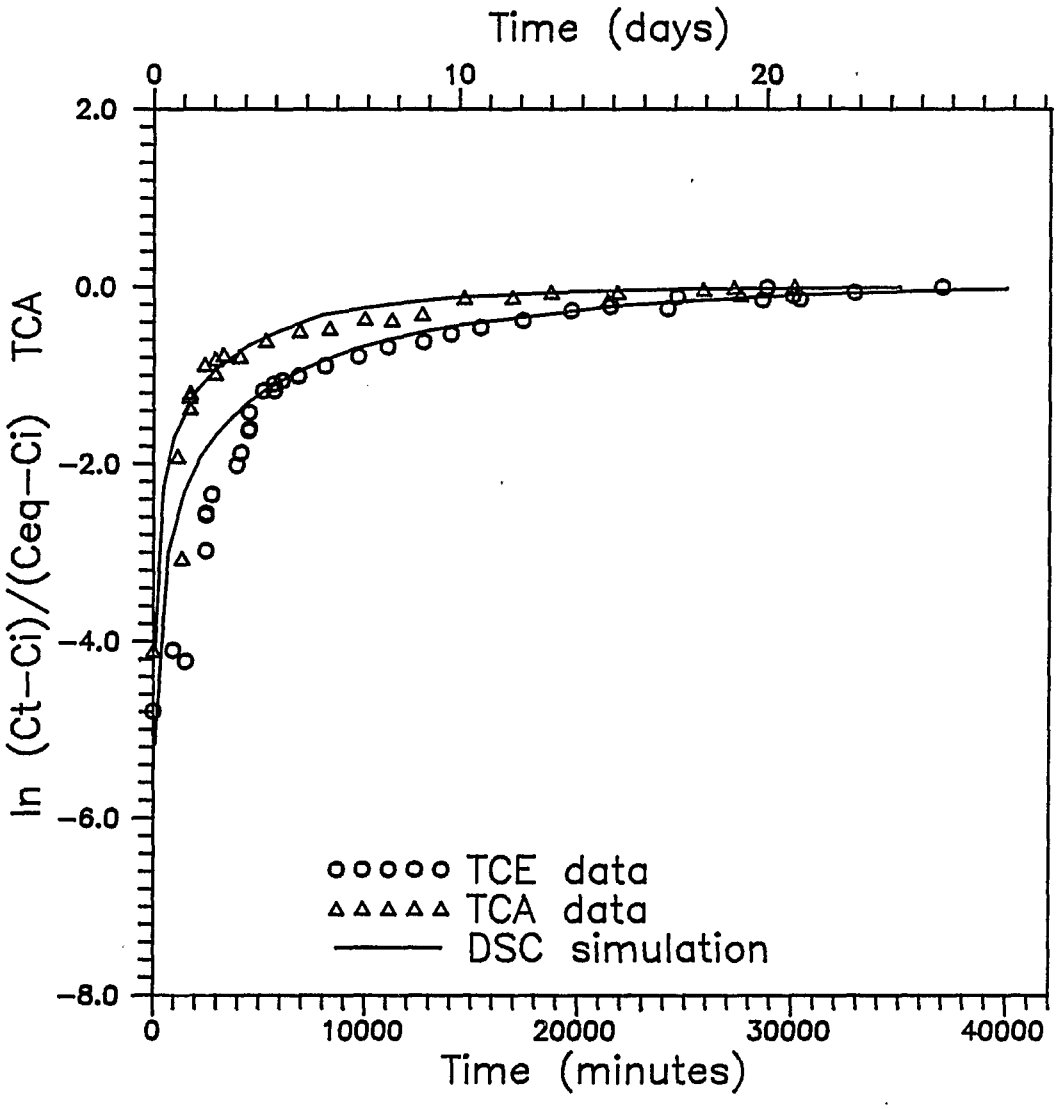

Figure 5.8. The measured solid-liquid-vapor mass transfer is compared to mass transfer simulated by the DSC model.

5.5 AIR STRIPPING SIMULATION

The air stripping simulation was based on the hypothesis that the process was controlled by mass transfer between the solid, liquid, and vapor phases in response to an imposed concentration gradient. The model was a compilation of the conservative tracer simulation, which modeled hydrodynamic dispersion, and the mass transfer algorithms discussed in 5.3 and 5.4.

Assuming that a VOC exists in the dissolved, solid, and vapor phases in unsaturated soil (no free product present), the fraction of mass in each phase can be written by:

$$C_l\Theta_s/(C_l\Theta_s + S\Omega_b + C_a\Theta_a) + \quad (5.4)$$
$$S\Omega_b/(C_l\Theta_s + S\Omega_b + C_a\Theta_a) +$$
$$C_a\Theta_a/(C_l\Theta_s + S\Omega_b + C_a\Theta_a) = 1$$

where

Θ_s = water filled porosity
(cm^3 water cm^{-3} porous media)

Θa = air filled porosity
(cm^3 air cm^{-3} porous media)

Ω_b = soil bulk density
(g soil cm^{-3} porous media)

C_a = vapor concentration (mg cm^{-3}air)

and $C_a = C_l H_c$ (mg cm^{-3} air)

$S = K_p C_l$ (mg g^{-1} soil)

To assign relative volumes to each cell, the fraction of air, liquid, and soil existing in the advecting and confining layers was first calculated. They are shown in Table 5.1.

SYSTEM CHARACTERISTICS	ADVECTING	CONFINING
Percent soil water	78	22
Percent soil air	92	8
Percent organic carbon	85	15

Table 5.1. The fraction of water, air, and organic carbon which each soil type contributed to the laboratory model.

The results of Equation 2.7 were then multiplied by the corresponding system fraction of soil, liquid, or air, (depending on the soil type). The value was then normalized with the volume of cell 1 so the vapor cells in the advecting layer were the same size used in the conservative tracer simulation. The saturated solid - liquid partitioning coefficient was varied to calibrate the DSC model simulation. This was done to try to account for partitioning to the adhesive and plexiglass. The fitting parameter will be referred to as C_f (correction factor).

Figure 5.9 is an illustration of the flow chart used in the simulation. The cell numbers correspond to those used in the computer program.

Table 5.2 records the multi-phase mass distribution of TCE used in the computer simulation for a Kp value of 0.165. Kp for TCE was increased by a factor of 3 to produce a correction factor. Increasing the Kp value caused a greater fraction of mass to be stored in the solid phase.

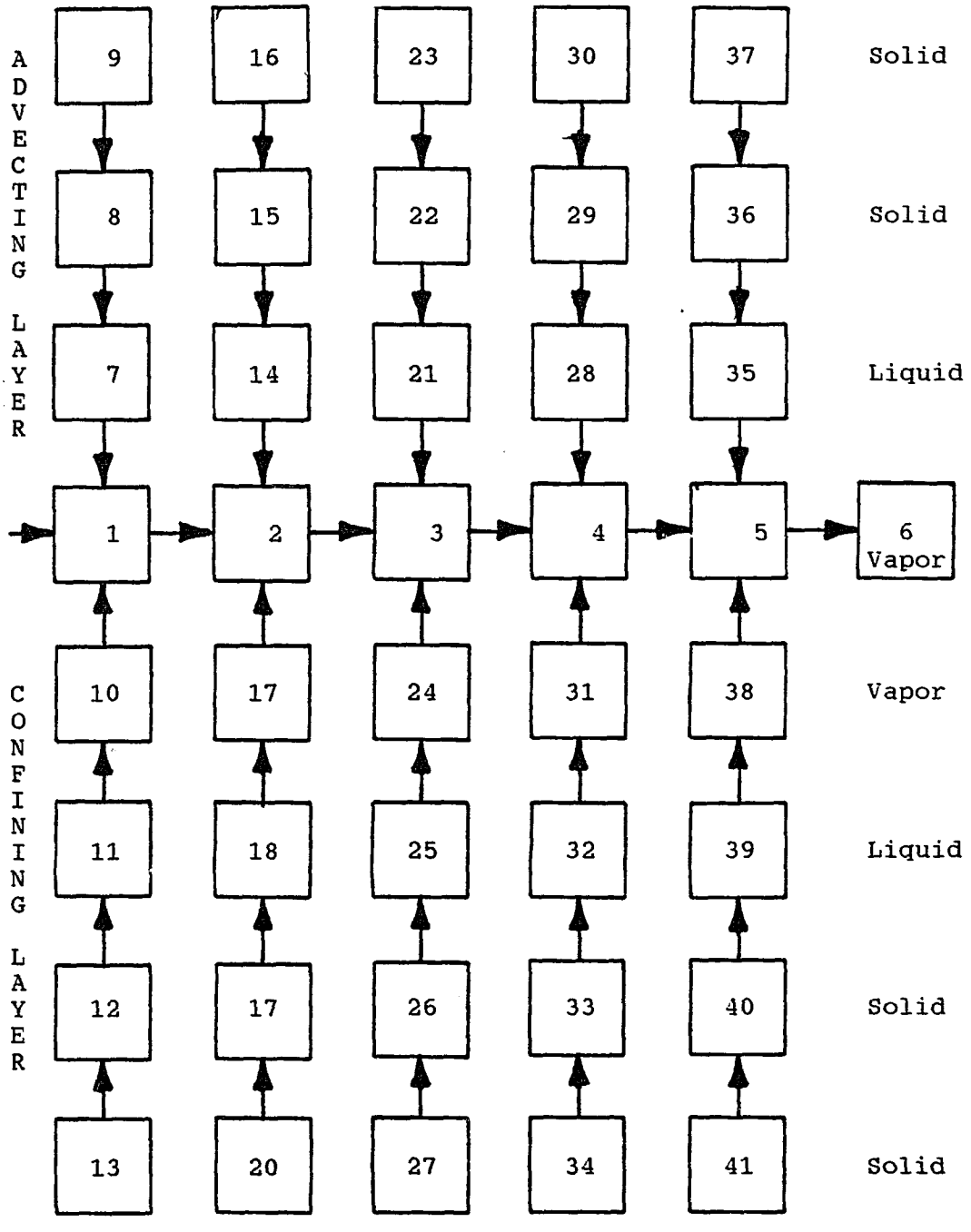

Figure 5.9. Flow chart used in air stripping simulation.

TCE MULTI-PHASE MASS DISTRIBUTION FOR COMPUTER SIMULATION

Solid - Liquid Partitioning Value	Phase	Percentage in Confining Layer	Percentage in Advecting Layer
	Liquid	44.9	30.3
Kp = 0.165	Vapor	8.1	17.3
	Solid	47.0	52.4
	Liquid	23.1	14.8
Cf = 0.495	Vapor	4.2	8.5
	Solid	72.7	76.7

Table 5.2. When Kp is increased to produce correction factors the multi-phase mass distribution of TCE is changed to reflect greater storage in the solid phase.

The DSC model was used to simulate the air stripping process in unsaturated soil. Initially, the VOC solid, liquid, and vapor phases were assumed to be in equilibrium. Advective transport of clean air caused a concentration gradient and induced mass transfer from liquid to vapor, and from solid to liquid. The solid - liquid partitioning coefficient, Kp(sat), was estimated for a saturated system using Equation 2.6. The calculated Kp value was 0.165 for TCE. The model was run using the Kp value and variable flow used in the experiment. The model was adjusted to account for variable flow, and the results are presented in Figure 5.10. The changes in flow rate are recorded below the graph.

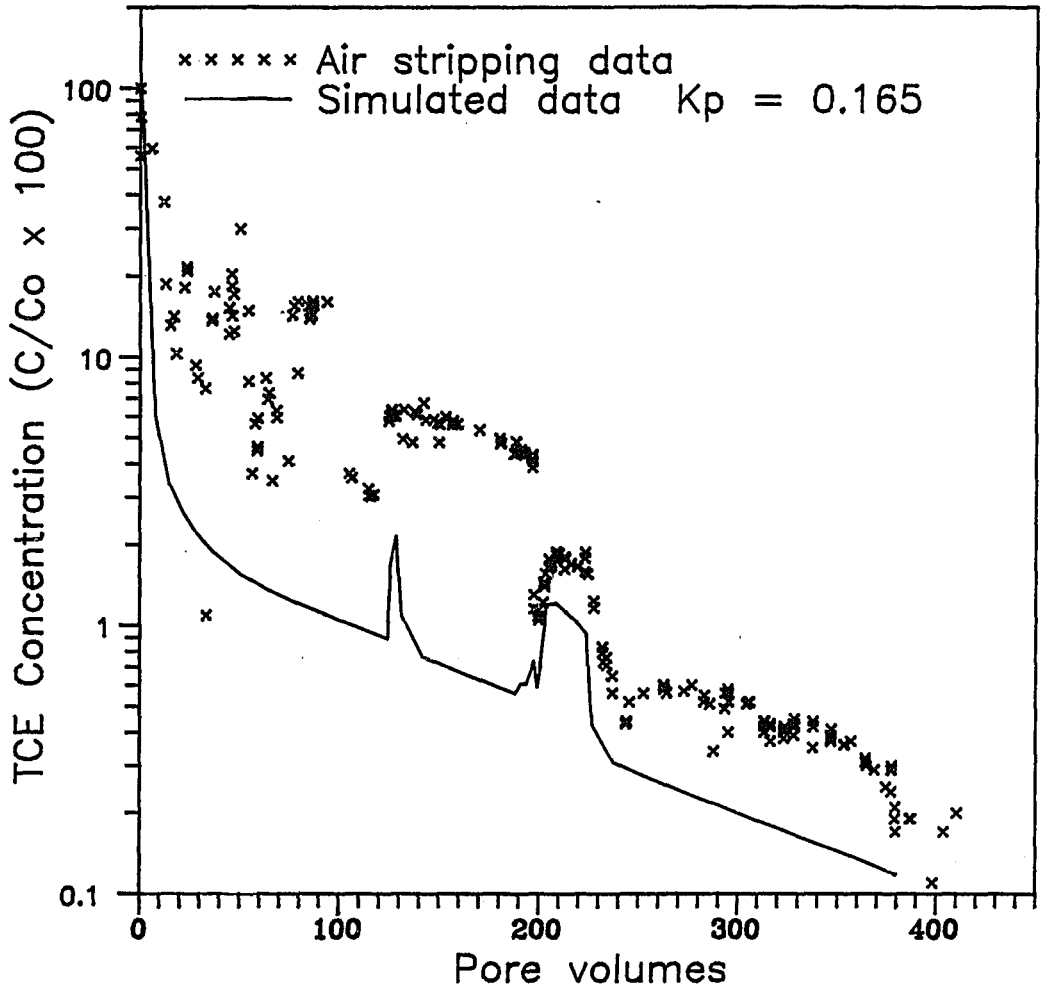

Pore Volumes	Flow (ml/min)	Pore Volumes	Flow (ml/min)
0.0 - 3.6	148	197.8 - 199.5	400
3.6 - 124.5	400	199.5 - 201.1	250
124.5 - 128.7	140	201.1 - 224.0	140
128.7 - 188.5	400	224.0 - 382.1	400
188.5 - 194.1	348	382.1 - 384.0	700
194.1 - 196.9	285	384.0 - 391.4	400
196.9 - 197.8	250	391.4 - 410.4	700

Figure 5.10. Variable flow DSC simulation is compared to the experimental data using the estimated solid - liquid partitioning value of 0.165.

After 200 pore volumes the model simulates the correlation between flow rate and vapor concentration, and the desorption trend measured in the laboratory.

Early in the experiment, the model predicts vapor concentration to drop much more rapidly than supported by the data. For a given volume of air removed, lower vapor concentration translates to less mass removed from the system. Therefore, a large fraction of mass removed early in the experiment is not accounted for by the model. To release sustained high concentrations of VOCs during the early part of the experiment, a solid - liquid mass transfer rate faster than the measured rate is required. The mass transfer rate was measured after the air stripping experiment had been completed when the sorbed concentration was low. A faster initial solid - liquid mass transfer rate would help explain the model discrepancy. A faster initial rate would cause more contaminant to be released early in the experiment, and keep vapor concentration high. The faster initial rate hypothesis could be tested by halting forced ventilation early in the experiment and measuring the increase in vapor concentration when the sorbed concentration is high.

The simulated effluent vapor concentration is lower than the experimental data using Kp = 0.165. The correction factor, C_f = 0.495, was introduced to account for sorption to the adhesive and plexiglass walls of the model. This indicates the potential importance of partitioning to these

surfaces. The model was run again with the correction factor. Introducing C_f changed the mass distribution by storing more mass in the solid phase. Mass in the liquid and vapor phases was held constant. Figure 5.11 compares the simulation to the experimental data using the correction factor.

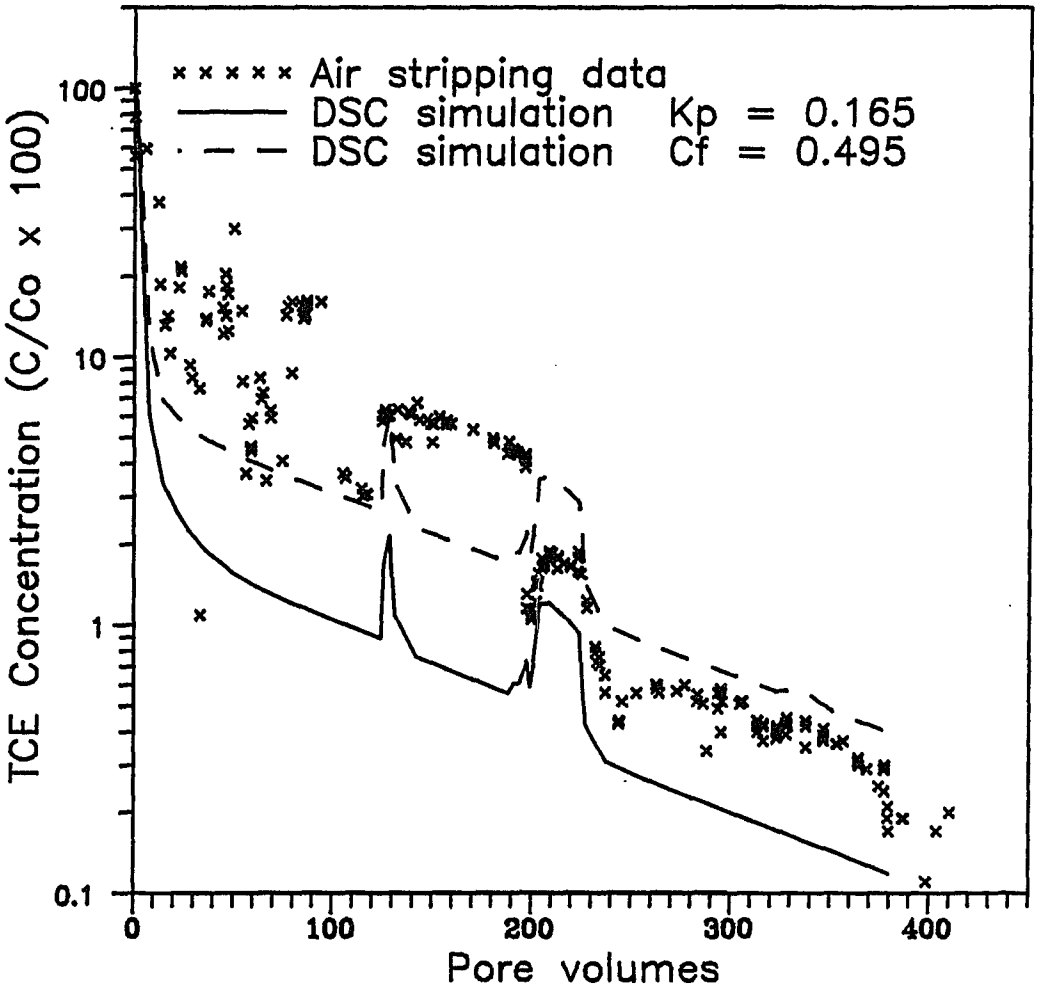

Pore Volumes	Flow (ml/min)	Pore Volumes	Flow (ml/min)
0.0 - 3.6	148	197.8 - 199.5	400
3.6 - 124.5	400	199.5 - 201.1	250
124.5 - 128.7	140	201.1 - 224.0	140
128.7 - 188.5	400	224.0 - 382.1	400
188.5 - 194.1	348	382.1 - 384.0	700
194.1 - 196.9	285	384.0 - 391.4	400
196.9 - 197.8	250	391.4 - 410.4	700

Figure 5.11. Variable flow DSC simulation is compared to the experimental data using Kp (0.165) and a correction factor value of 0.495.

Since the source of 1,1,1-TCA was the adhesive used to glue sand to the laboratory model, an estimate of mass sorbed onto the soil would be negligible compared to storage in the adhesive. Figure 5.11 compares the simulation using Kp = 0.135 to the air stripping data. The large disparity indicates an underestimation of mass in the solid phase. The model simulates the desorption trend, and displays the correlation between flow rate and vapor concentration. Early in the experiment the simulation predicts vapor concentration to drop faster than the data support, and, therefore, the mass removed from the system is underestimated.

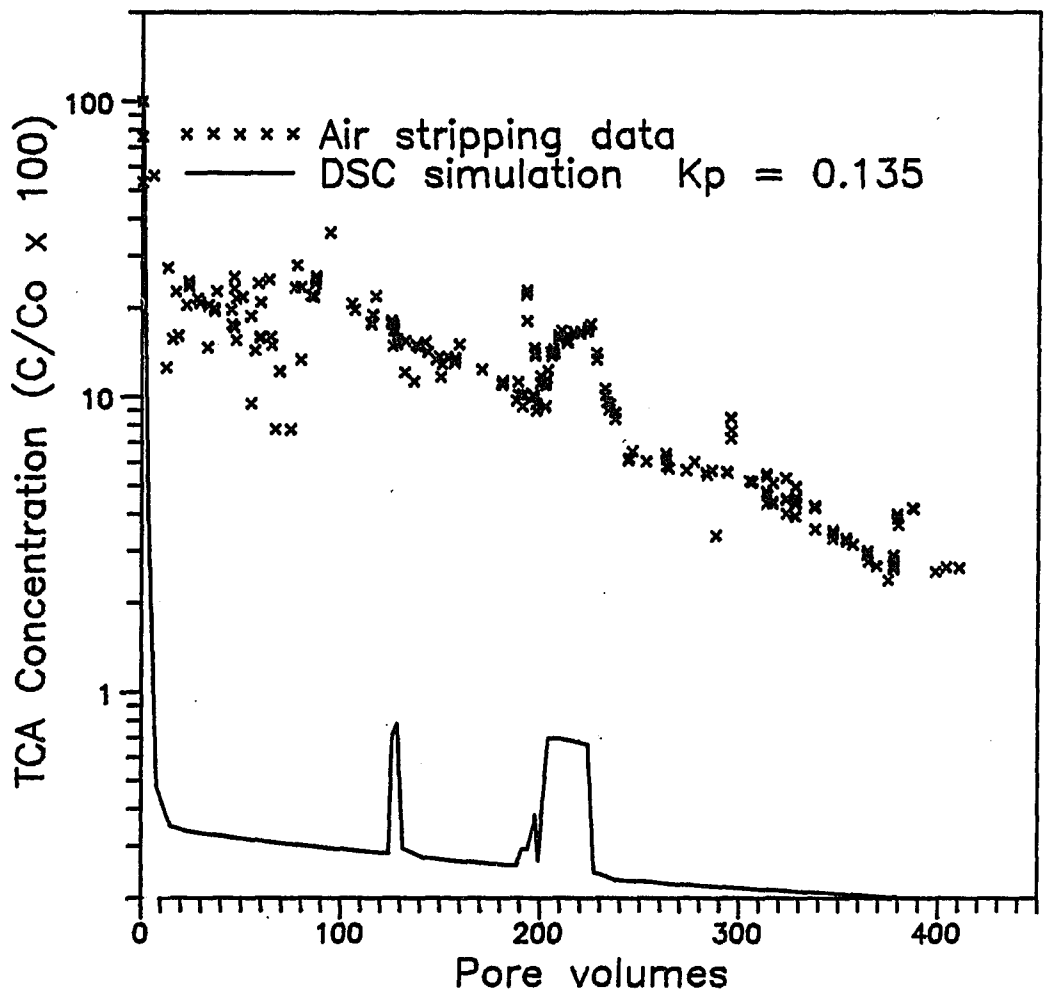

Pore Volumes	Flow (ml/min)	Pore Volumes	Flow (ml/min)
0.0 - 3.6	148	197.8 - 199.5	400
3.6 - 124.5	400	199.5 - 201.1	250
124.5 - 128.7	140	201.1 - 224.0	140
128.7 - 188.5	400	224.0 - 382.1	400
188.5 - 194.1	348	382.1 - 384.0	700
194.1 - 196.9	285	384.0 - 391.4	400
196.9 - 197.8	250	391.4 - 410.4	700

Figure 5.12. Variable flow DSC simulation compared to 1,1,1-TCA air stripping data Kp = 0.135 indicates most of the solid phase storage is in the adhesive.

6. CONCLUSIONS AND RECOMMENDATIONS FOR FURTHER STUDY

6.1 HELIUM TRACER EXPERIMENTS

The laboratory model produced a pressure field which conformed with the governing fluid flow equation in radial coordinates (Equation 2.10). A mixture of helium and air was used to approximate a conservative gas phase tracer, and tests indicated that preferential flow paths did not exist. Tailing in the measured breakthrough curves may indicate He diffusion between the advecting layers and confining layers as well as He dissolution in soil moisture. The measured He breakthrough curve was similar to the simulation, and provided a good approximation for a conservative breakthrough curve. There were many advantages for using He as a gas phase tracer. It is environmentally innocuous, chemically inert, easy to detect in small concentrations, and inexpensive.

6.2 AIR STRIPPING EXPERIMENTS

This investigation attempted to show that air stripping in unsaturated soil can be characterized by mass transfer between the sorbed, dissolved, and vapor phases in response to an imposed concentration gradient. Estimation of the liquid - vapor mass transfer rate with batch experiments showed rapid equilibration between the dissolved and vapor

phases. Batch test equilibrium was accomplished in about 35 minutes. The residence time of the advecting air ranged from 80 to 400 minutes which allowed adequate time for liquid - vapor equilibration. Similar vapor concentration in the headspace of aqueous samples, and the laboratory model effluent confirmed near equilibrium conditions.

The solid - liquid - vapor mass transfer rate was determined in situ by halting forced ventilation, and measuring the increase in vapor concentration with time. The overall mass transfer rate was about 3 orders of magnitude slower than liquid - vapor desorption alone. The measured mass transfer rates were used to calibrate the DSC model. The DSC model simulated the desorption trend, and the correlation between flow rate and vapor concentration during the last half of the experiment. It underestimates the early sustained removal of VOCs in high concentrations. The solid - liquid - vapor mass transfer rate was measured after the 47 day air stripping experiment, and may be slower than the rate in effect when air stripping was initiated. It may be that VOCs are loosely bound to soil minerals or organic matter when the sorbed concentration is high. If VOCs were initially released at a faster rate from the solid phase it would help explain the rapid release of mass early in the experiment.

In situ measurement of vapor re-equilibration after a period of airstripping characterizes the overall VOC mass transfer. The rate encompasses desorption from the solid

phase to liquid, vaporization from the dissolved phase, and diffusion of VOCs through soil aggregates. The overall mass transfer rate describes the accumulation of vapor in the soil pore space and, therefore, the data can be used for predicting VOC removal during air stripping. The overall mass transfer characteristics were simulated with the DSC model in this investigation. The data could also be applied to other methods which couple mass transfer reactions with the advection - dispersion equation.

The DSC model shows promise for simulating air stripping in unsaturated soil. Equilibrium partitioning coefficients, and mass transfer measurements are necessary to properly calibrate the model. When calibrated, the DSC model could be used to evaluate alternative pumping strategies. Figure 6.1 compares extraction at a constant flow rate to pulse extraction at an equivalent rate.

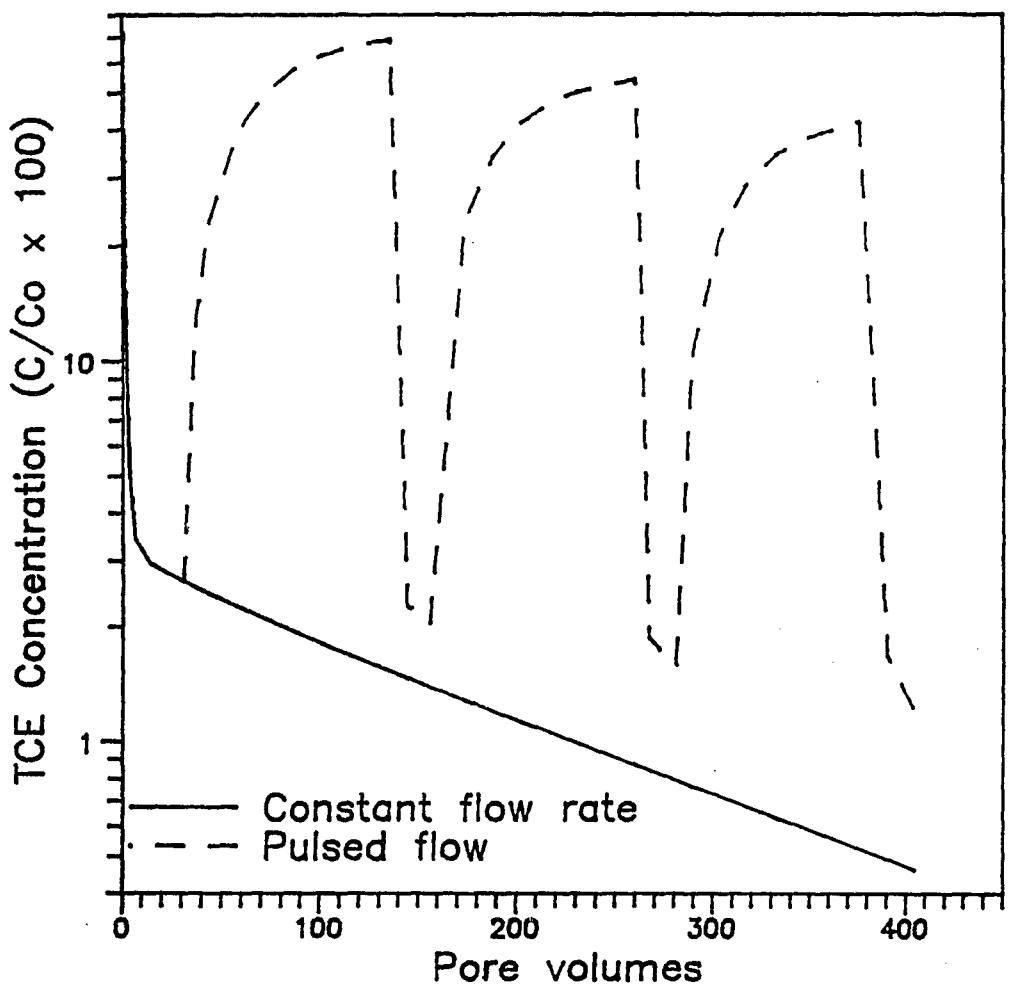

Figure 6.1. Extraction at a constant flow rate compared to pulsed extraction at an equivalent flow rate.

6.3 COLUMN EXPERIMENT

A smaller laboratory experiment is proposed in which a glass column reactor filled with soil material. The use of a glass column would prevent VOC sorption to the laboratory apparatus. Soil material could be natural, or synthetic (i.e., silica sand coated with humic acid). Suction candles could be used as before to establish a unit gradient, and to facilitate aqueous sampling. Soil vapor could be more effectively monitored because the length of tubing from the syringe septa to the sampling port would be reduced.
Helium tracer tests could be conducted more quickly in the column reactor, and modeled with out the complication of radial geometry.

The parameters needed for the DSC model are equilibrium partitioning coefficients and amounts of soil, water, and air, and organic carbon in the system. Henry's constant is a reliable estimate of the liquid - vapor partitioning coefficient for compounds that form dilute solutions with water. The Kp could be calculated if a careful mass balance was obtained during VOC injection. This value could be compared to estimates of Kp obtained from regression equations based on soil fraction organic content. Liquid - vapor mass transfer rates can be measured in batch experiments as before. Another approach would be to use a column of clean silica sand to eliminate the influence of sorption to the solid phase. Forced ventilation could be halted after a

period of air stripping establishes nonequilibrium conditions, and the rate of change of vapor concentration in the column could be measured. The solid - liquid - vapor mass transfer rate could be measured in a similar manner. A rate measured early in the air stripping history should be compared with a later rate to see if mass transfer is faster when the sorbed concentration is high.

6.4 SOIL LAYERING

VOC diffusion between the advecting and confining layer was not rigorously considered in this study. More experiments are needed to determine the potential for low permeable layers to retain high concentrations of VOCs, and to develop strategies to remediate them.

7. APPENDIX A

USERS MANUAL: DISCRETE STATE COMPARTMENT MODEL

The Discrete State Compartment (DSC) model was originally proposed by Dr. Eugene S. Simpson of the University of Arizona while he was on sabbatical leave at the International Atomic Energy Commission in Vienna, Austria during 1971. The computer code for the DSC model was initially written in FORTRAN 4 by Michael E. Campana at the University of Arizona in 1975. The program has been substantially re-written in FORTRAN 77 for the purpose of execution on the IPM-PC and compatible micro-computers.

A.1 Operation of the Discrete State Compartment Model

A hydrologic system may be represented by a network of compartments (also called cells) so that variations in flows and concentrations of solutes within the system may be understood and modeled. The model can be used to simulate flow in a number of compartments, each of which can vary in volume, prorosity, geometry, and diffusivity. The program has also been developed for applications where the compartments contain a fixed volume during all iterations, as well as problems of non-steady volume.

A recursive equation is written so that inputs, outputs, as well as sources and sinks within compartments are combined. The recursive equation maintains mass balances to conserve the equation of continuity. The basic equation used by the DSC model is:

(A.1) $S(n,t+1) = S(n,t) + BRV(n,t)*BRC(n,t) - BDV(n,t)*BDC(n,t) + R(n,t)$

where $S(n,t)$ = mass of solute in cell n at time iteration t

$BRV(n,t)$ = boundary recharge volume (input volume of water to cell),

$BRC(n,t)$ = boundary recharge concentration (input concentration of solute),

$BDV(n,t)$ = boundary discharge volume (output volume of water from cell),

$BDC(n,t)$ = boundary discharge concentraction (output concentration of solute), and

$R(n,t)$ = sum of solute sources and/or sinks within the cell

The advection-diffusion equation (see Freeze and Chery, 1980) is solved by employing two different mixing schemes. The solution is obtained by decomposing the advection-diffusion equation into an advection scheme, and a

separate diffusion scheme. The advection scheme is appropriate when the movement of fluid and solutes from one compartment to another occurs as the result of a fluid velocity field. The velocity field results from a gradient of potential within the fluid. The diffusion scheme is appropriate when the movement of solutes occurs when a gradient of solute concentrations is present. The two schemes can be combined for applications where both processes occur simultaneously. A discussion of the advection and diffusion algorithms is presented in the next sections.

A.1.1 Advection Algorithms

Two alternate algorithms are available for solving the boundary discharge concentration (BDC) from each compartment or cell as the result of advection. The first equation is termed the Simple Mixing Cell (SMC) algorithm. The BDC at each time step is obtained by assuming that at each iteration the cell walls expand to accommodate the incoming water (Figure 1, upper illustration). The incoming water and solutes completely mix with the contents of the cell. Following that, the cell walls contract to their original volume and the cell discharges a volume of water equal to the volume which entered. The BDC will be equal to the concentration in the cell in its expanded condition. The operation may be described as a 'input-mix-output' scheme. The BDC is found from:

(A.2) $BDC(n,t+1) = S(n,t) + BRV(n,t)*BRC(n,t)/[VOL(n,t) + BRV(n,t)]$

where $VOL(n,t)$ = the volume of cell n for iteration t.

Alternatively, the model can solve for the BDC using a modified mixing cell (MMC) algorithm which assumes that at each iteration the incoming water first displaces a volume of cell water equal to the incoming volume, and then the incoming water mixes with the remaining cell contents (Figure 1, lower illustration). The operation is an 'input-output-mix' scheme and the BDC can be calculated from:

(A.3) $BDC(n,t+1) = S(n,t) / VOL(n,t)$

A.1.2 Exchange Algorithm

Additionally, an exchange algorithm has been incorporated into the model which allows for modeling processes where no water transport is observed. The algorithm allows for such processes as heat and solute movement as the result of conduction and diffusion, respectively. Because no movement of solvent need occur, the solute can be modeled without any net movement of water. Again there are two possibilities for exchange. Using the SMC algorithm, a volume of water and tracer is first moved from one cell and mexed with the next (Figure 2, upper illustration). After mixing, an equivalent

amount of water and the new concentration of tracer are moved back to the original cell and mixed. The operation would be an 'input-mix-output-mix' scheme. The operation can be described analytically by taking the difference between the mass transported from the first cell to the second cell and subtracting the mass transported back from the second cell to the first as indicated by:

(A.4a) $M_1 = XV * S(1,t) / VOL(1)$

(A.4b) $M_2 = XV * (M_1 + S(2,t)) / (XV + VOL_2)$

(A.4c) $M = M_1 - M_2$

$= XV*(S(1,t)/VOL(1) - [S(1,t)/VOL(1) + S(2,t)]/(XV + VOL_2))$

where XV = exchange volume transported from the first cell to the second and then back to the first,

M_1 = mass transported from cell 1 to cell 2,

M_2 = mass transported from cell 2 to cell 1, and

M = net mass flux between the two cells.

The second option uses the MMC algorithm to calculate the mass flux. In this case the operation would be to exchange equal volumes before mixing and then to mix after

the exchanges take place (Figure 2, lower illustration). The procedure would be an 'input-output-mix-mix' scheme, as indicated below:

(A.5a) $M_1 = XV * S(1,t) / VOL(1,t)$

(A.5b) $M_2 = XV * S(2,t) / VOL(2,t)$

(A.5c) $M = XV * [S(1,t) / VOL(1,t) - S(2,t) / VOL(2,t)]$

A.1.3 Radioactive Decay

An algorithm is included within the program which reduces the mass of a solute by a factor proportional to the mass within the cell. This can be obtained by calculating a time step dependent decay factor, RD:

(A.6) $RD = \exp(\ln(1/2) * dt / T_{1/2})$

where $T_{1/2}$ = isotope half-life, and

dt = real-time interval of each iteration

The updated state of each cell is calculated using the decay factor:

(A.7) $S(n,t+1) = RD * S(n,t)$

A.1.4 First Order Kinetic Reactions

The sorption of a solute into an immobile phase may occur at rates such that an instantaneous equilibration can not be assumed. In this case, a kinetic term is used to relate the rate of change of the solute to the concentration of the solute, according to (Rasmussen, M.S. Thesis, Hydrology and Water Resources, University of Arizona, 1982):

A.1.5 Non-steady volume

In the previous sections the assumption is made that the amount of inflow to a cell is equal to the amount of outflow. In certain applications the modeler may wish to vary the volume of the cells or of individual cells. In particular, the use of linear reservoir may be required. To allow for this case, the program contains the option for determining the outflow from a cell as a function of the storage within the cell. The parameter within the DSC model which determines the rate of discharge is FAC and is used as follows:

(A.8) $$FAC(n) = VOL(n,t) / BDV(n,t)$$

A threshold parameter, PHI, is also included so that discharge is not allowed to occur until the storage exceeds the threshold value. This may be written as:

$$BDV(n,t) = [VOL(n,t) - PHI(n)] / FAC(n) \quad \text{for } VOL(n) > PHI(n)$$

A.1.6 Calculation of Ri for diffusion

The calculation of Ri for diffusion is different from advective flow where Ri is the fraction of the output transported to a cell. In the exchange algorithm Ri is the volume exchanged between two cells and is calculated from Fick's Law. The process of diffusion can be described mathematically using Fick's Law. If Fick's Law is approximated by a finite time interval, #n, then the following equation can be written:

$$M_1 - M_2 = D\ (C_1 - C_2)\ /\ \#x\ A\ \$\ \#t$$

where $M_1 - M_2$ = mass transported across the interval #x

A = cross-sectional area normal to #x

$ = porosity

C_1, C_2 = discrete concentrations

D = coefficient of molecular diffusion

By setting the net mass flow obtained by means of Fick's Law to the net mass flow obtained in the two exchange algorithms, the relationship between D and Ri can be established. For the SMC the relationship is:

$$Ri = (Vol_2\ D\ A\ \$\ \#n)\ /\ Vol_1\ (Vol_2\ \#x - D\ A\ \$\ \#n)$$

For the MMC it is:

$Ri = D\ A\ \$\ \#n\ /\ Vol_1\ \#x$

A.2 Entry of Data for DSC Model

A brief description of the data requirements for the program is presented below. The program requires a minimum of 13 input lines of data. There may also be continuation lines when the required input data exceeds 80 columns. There may also be additional lines when optional input data is required. The required format of the data is presented after the input line number.

Input line 1 - Format 8i10

NCEL - The total number of cells in the system

ICEL - The number of cells receiving inputs from outside the system. These cells must be numbered consecutively starting with number 1 through ICEL.

NIT - The total number of iterations.

KZ - The number of columns in the K-rout table and number of elements in RI.

MAGE - Set equal to 1 if you want the mean and variance of the age distribution calculated by the impulse-response method, otherwise set equal to 0.

KCELL - If you want the age distributioncalculated here you must specify which cells.

KITER - Iterations you would like age distribution calculated for.

MATDIR - Set equal to 1 if you want mean ages for cells calculated by the direct matrix method.

Input line 2 - Format 8i10

ITYPE - If simple mixing cell (SMC) algorithm is desired for routing advective flows, set ITYPE = 0 or leave blank. If the modified mixing cell (MMC) algorithm is desired, set ITYPE = 1.

JTYPE - If simple mixing cell (SMC) algorithm is desired for routing exchange flows, set Jtype = 0 or leave blank. If the modified mixing cell (MMC) algorithm is desired, set ITYPE = 1.

IFvar - If constant volumes are desired for each iteration, set IFvar = 0 or leave blank. For the non-steady volume regime (as modeled by a linear, time-invariant reservoir algorithm) set IFvar = 1.

MassIN - Set this variable = 1 to have cell states read in with mass dimensions. For concentration dimensions, set this MassIN = 0 or leave blank.

IFprin - Total number of iterations at which data printouts are desired. If printouts are desired at each iteration, set IFprin = -1.

IFsbrv - If the same system boundary recharge volume, SBRV, is to be used at each iteration, set IFsbrv = 0. If a specific number of changes are desired (after the first), set IFsbrv equal to the number of changes desired. As a dimension

in the program only 11 changes in the sbrv can be made.

IFsbrc - Parameter similar to IFsbrv, except that IFsbrc pertains to the set of system boundary recharge concentrations, SBRC. IFsbrc is determined in the same manner as IFsbrv.

Optional input lines following line 2 - Format 8i10

(Each variable must be on its own input line.)

ITprin - If IFprin > 0, read the array storing the specific iteration numbers (in ascending order) at which data printouts are desired.

ITsbrv - If IFsbrv = 1, read the array storing the specific iteration numbers (in ascending order) at which changes in the set of system boundary recharge volumes are to be made.

ITsbrc - If IFsbrc = 1, read the array storing the specific iteration numbers (in ascending order) at which changes in the set of system boundary recharge concentrations are to be made.

CELLNUM - If KCELL is greater than 0, read the array storing the cell numbers you would like age distribution calculated.

CELLIT - If age distribution is to be calculated list iteration numbers in ascending order at which it will be.

Optional input lines following line 2 - Format 8f10.3

FAC - If IFvar = 1, read FAC(NCEL), the array storing the non-steady volume factors. If FAC(J) equals zero, then a

steady volume regime is specified for cell J. If cell J undergoes pure exchange only, FAC(J) equals zero.

PHI - If IFvar = 1, read PHI(NCEL), the array of cell threshold volumes for the linear reservoir algorithm. These volumes can be zero if no thresholds are desired. A cell will not be allowed to discharge until its volume exceeds the threshold volume.

Input line 3 - Format 8f10.3

Half - The half-life of the solute. If not required set to 0, or leave blank

Delta - Time between iterations. Time can be expressed in terms of a unit-reference time. Any time units can be used as long as consistency is maintained throughout the program.

Date - Initial starting time. If not required set to 0, or leave blank.

SBRconc - Needed when running either of the mean age algorithms. It is equal to the initial SBRC.

Input line 4 - Format 8f10.3

STATE - Read the initial mass (or concentration). Initial masses can have either concentration or proper state dimensions (see MassIN).

Input line 5 - Format 8f10.3

Volume - Read the initial volume of each cell. All volumes

are expressed as multiples of a unit reference volume. These volumes will remain constant unless a non-steady volume regime is specified (see IVAR).

Input line 6 - Format 8f10.3

SBRV - Read in the initial system boundary regharge volumes. Other SBRV data may be read later. Only the first ICEL cells can reveive SBRV's.

Input line 7 - Format 8f10.3

SBRC - Read in the initial system boundary recharge concentrations, SBRC. Other SBRC data can be read later. Only the first ICEL cells can receive SBRC's.

Input lines 8, 9, and 10 - Format 20i4

Krout - The K-rout table is used to define the flow paths within the cell model. The table is divided into three sets: Line 9 lists the "from" cells, while line 10 lists the "to" cells. Card 11 indicates whether the transfer is an advective flow (indicated by a zero, or a blank) or whether the transfer is an exchange (indicated by a 1). If a cell is receiving an input from outside the system, a zero or a blank is place in the "from" cell position. All cells receiving inputs from outside the system must be consecutively beginning with 1 (i.e., cells 1 through Icel are the first Icel entries in this table). Before a cell can discharge some of its contents, all

inputs to that cell must be listed. In the case of an exchange, all non-exchange inputs to both cells should be listed before the exchange occurs. If this is not possible, all non-exchange inputs to the cell depicted as discharging its exchange volume first should be listed before the exchange occurs.

Input line 11 - Format 8f10.3

RI - One may consider the RI array to be the fourth row of the K-rout table. RI contains the fraction of the output of the "from" cell (indicated in line 9) that flows to the "to" cell (indicated in line 10). If an exchange occurs between two cells, then the fraction of volume of the first cell which is to be transfered between the two cells is placed in the RI array.

Optional input lines following line 12 - Format 8f10.3

SBRV - Read in additional SBRV data, see IFsbrv.

Optional input lines following line 12 - Format 8f10.3

SBRC - Read in additional SBRC data, SEE IFsbrc.

8. REFERENCES

Amy, G.L., R.M. Narbaitz, and W.J. Cooper, 1987, "Removing VOCs from groundwater containing humic substances by means of coupled air stripping and adsorption", American Water Works Association Journal, 76(5): 49-54.

Ball, W.P., M.D. Jones, and M.C. Kavanaugh, 1984, "Mass transfer of volatile organic compounds in packed tower aeration", Journal of Water Pollution Control Federation, 56: 127-136.

Bruckner, F., H.M. Harress, and D. Hiller, 1986, Brunnenbauhrleitungsbau, 37: 174-179.

Handbook Of Chemistry And Physics, The Chemical Rubber Company, Cleveland, Ohio, 1973.

Chiou, C.T., and T.D. Shoup, 1985, "Soil sorption of organic vapors and effects of humidity on sorptive mechanism and capacity", Environmental Science and Technology, 12: 1196-1200.

Cline, C.C., T.J. Lane, and M. Saldamando, 1985, "Packed column aeration for trichloroethylene removal at Scottsdale, Arizona", Annual Conference Proceedings of American Water Works Association, 1083-1099.

Crow, W.L., E.P. Anderson, and E.M. Mingh, 1987 "Subsurface venting of vapors emanating from hydrocarbon product on ground water", Ground Water Monitoring Review, Winter 1987: 51-57.

Dowd, R.M., 1984, "Leaking underground storage tanks", Environmental Science and Technology, 18: 309A.

Freeman, D.H., and L.S. Cheung, 1981, "A gel partition model for organic desorption from a pond sediment", Science, 214: 790-792.

Freeze, R.A., and J.A. Cherry, 1979, Groundwater, Prentice-Hall, Inc., Englewood Cliffs, New Jersey, 604 pp.

Gossett, J.M., 1987, "Measurements of Henry's law constants for C1 and C2 chlorinated hydrocarbons", Environmental Science and Technology, 21: 202-208.

Hand, D.W., J.C. Crittenton, J.L. Gehin, and B.W. Lykins, Jr., 1986, "Design and evaluation of an air-stripping tower for removing VOCs from groundwater", American Water Works Journal, 32: 180-186.

Hillel, D., 1980, Fundamentals Of Soil Physics, Academic Press, Inc., Orlando, Florida, 413 pp.

Hoag, G.E., A.L. Baehr, and M.C. Marley, 1987, "In-situ recovery of hydrocarbon contaminated soil utilizing the induced soil venting process", International Conference, March 1987, Vienna, Austria.

Horvath, A.L., 1982, Halogenated Hydrocarbons, Solubility-Miscibility With Water, Marcel Dekker, Inc., New York.

Karickhoff, S.W., 1980, "Sorption kinetics of hydrophobic pollutants in natural waters", Contaminants and Sediments, Vol. 2 (ed. R.A. Baker), Ann Arbor Science Publishers, Inc., Ann Arbor, Michigan, pp. 193-205.

Karickhoff, S.W., 1984, "Organic pollutant sorption in aquatic systems", Journal of Hydraulic Engineering, 110: 707-735.

Kilbury, R.K., T.C. Rasmussen, D.D. Evans, and A.W. Warrick, 1986, "Water and air intake of surface-exposed rock fractures in situ", Water Resources Research, 22: 1431-1443.

Leenheer, J.A., and J.L. Ahlrichs, 1971, "A kinetic and equilibrium study of the adsorption of carbaryl and parathion upon soil organic matter surfaces", Soil Science Society of America Proceeding, 35: 700-704.

MacKay, D., and P.J. Leinonen, 1975, Rate of evaporation of low-solubility contaminants from water bodies to atmosphere", Environmental Science and Technology, 9: 1178-1180.

Malcom, R.L., and P. MacCarthy, 1986, "Limitations in the use of commercial humic acids in water and soil research", Environmental Science and Technology, 20: 904-910.

Marley, M.C., 1985, Quantitative and qualitative analysis of gasoline fractions stripped by air from the unsaturated soil zone (M.S. Thesis), University of Connecticut, 87 pp.

Munz, C., and P.V. Roberts, 1987, Air-water phase equilibria of volatile organic solutes", Journal of the American Water Works Association, 79:5 62-69.

Muskat, M., 1946, The Flow Of Homogeneous Fluids Through Porous Media, J.W. Edwards, Inc., Ann Arbor, Michigan, 763 pp.

Peterson, M.S., L.W. Lion, and C.A. Shoemaker, 1988, "Influence of vapor-phase sorption and diffusion on the fate of trichloroethylene in an unsaturated aquifer system", Environmental Science and Technology, 22: 571-578.

Rasmussen, T.C., 1981, Solute Transport In Saturated Fractured Media, (Unpublished M.S. Thesis), University of Arizona, Tucson.

Roberts, M., 1987, Volatile Fluorocarbon Tracers For Monitoring Water Movement In The Unsaturated Zone, (Unpublished M.S. Thesis), University of Arizona, Tucson.

Roberts, P.V., and P.G. Dandliker, 1983, "Mass transfer of volatile organic contaminants from aqueous solution to the atmosphere during surface aeration", Environmental Science and Technology, 17: 484-489.

Schwarzenbach, R.P., and J. Westall, 1981, "Transport of nonpolar organic compounds from surface water to groundwater: Laboratory sorption studies", Environmental Science and Technology, 15:1360-1367.

Seidemann, R. H., 1988, Gaseous Transport In The Vadose Zone: Computer Simulations Using The Discrete State Compartment Model, (Unpublished M.S. Thesis), University of Arizona, Tucson.

Sleep, B.E., and J.F. Sykes, 1989, "Modeling the transport of volatile organics in variably saturated media", Water Resources Research, 25: 81-93.

Texas Research Institute, Inc., 1984, Forced Venting to Remove Gasoline Vapor From A Large Scale Model Aquifer, Final Report, American Petroleum Institute.

Thorton, J. S., and Wootan, W.L. Jr., "Venting for the removal of hydrocarbon vapors from gasoline contaminated soil", Journal of Environment, Science, and Health, 17:31-44.

Treybal, R.E., 1980, Mass Transfer Operations, McGraw-Hill Book Company, New York, New York, 784pp.

USEPA, 1980, The occurrence of volatile organics in drinking water, USEPA Briefing Paper, Office of Drinking Water, Cincinnati, Ohio.

Westenberg, A. A., and R. E. Walker, 1957, "New method of measuring diffusion coefficients of gases", Journal of Chemical Physics, 26:1753-1754.

Wu, S., and P.M. Gschwend, 1986, "Sorption kinetics of hydrophobic organic compounds to natural sediments and soils", Environmental Science and Technology, 20:717-725.